



The role of buoyancy forcing for northern North Atlantic SST variability across multiple time scales

Bjørg Risebrobakken¹, Mari F. Jensen², Helene R. Langehaug³, Tor Eldevik⁴, Anne Britt Sandø⁵, Camille Li⁴, Andreas Born², Erin L. McClymont⁶, Ulrich Salzmann⁷, Stijn De Schepper¹

¹NORCE Norwegian Research Center, Bjerknes Centre for Climate Research, Bergen, Norway

²Department of Earth Sciences, University of Bergen and Bjerknes Centre for Climate Research, Bergen, Norway

³Nansen Environmental and Remote Sensing Center, Bjerknes Centre for Climate Research, Bergen, Norway

⁴Geophysical Institute, University of Bergen and Bjerknes Centre for Climate Research, Bergen, Norway

⁵Institute of Marine Research, Bjerknes Centre for Climate Research, Bergen, Norway

⁶Department of Geography, Durham University, Durham, UK

⁷Department of Geography and Environmental Sciences, Northumbria University, UK

Correspondence to: Bjørg Risebrobakken (bjri@norceresearch.no)

Abstract: Analyses of observational data (from year 1870 AD) show that Sea Surface Temperature (SST) anomalies along the pathway of Atlantic Water transport in the North Atlantic, the Norwegian Sea and the Iceland Sea are in-phase at multidecadal time scales. In-phase SST anomaly relationships are also observed over hundreds of thousands of years during parts of the Pliocene (5.23–5.03, 4.63–4.43 and 4.33–4.03 Ma). However, when investigating CMIP6 SSP126 future scenario runs (next century) and Pliocene reconstructions (5.23–3.13 Ma), three additional phase relations emerge: 1) The Norwegian Sea is out of phase with the North Atlantic and the Iceland Sea (Pliocene; 4.93–4.73 and 3.93–3.63 Ma); 2) The Iceland Sea is out of phase with the North Atlantic and the Norwegian Sea (Pliocene; 3.43–3.23 Ma); 3) The North Atlantic is out of phase with the Norwegian and Iceland Seas (future trend). Hence, out of phase relationships seem to be possible in equilibrium climates (Pliocene) as well as in response to transient forcing (CMIP6 SSP 126 low-emission future scenario). Since buoyancy is a key forcing for inflow of Atlantic Water to the Norwegian Sea, we investigate the impacts of buoyancy forcing on the phase relation between SST anomalies in the North Atlantic, Norwegian and Iceland Seas. This is done by performing a range of idealized experiments using the Massachusetts Institute of Technology general circulation model (MITgcm). Through these idealized experiments we can reproduce three out of four of the documented phase relations: in-phase relationships under weak to intermediate fresh water forcing over the Nordic Seas; the Iceland Sea out of phase with the North Atlantic and the Norwegian Sea under weak atmospheric warming over the Nordic Seas; and the North Atlantic out of phase with the Norwegian and Iceland Seas under strong atmospheric warming over the Nordic Seas. We suggest that the unexplained phase relation, when the Norwegian Sea SSTs are out of phase with the North Atlantic and the Iceland Sea, may reflect a response to a weakened Norwegian Atlantic Current compensated by a strong Irminger current, or an expanded East Greenland Current.

1 Introduction

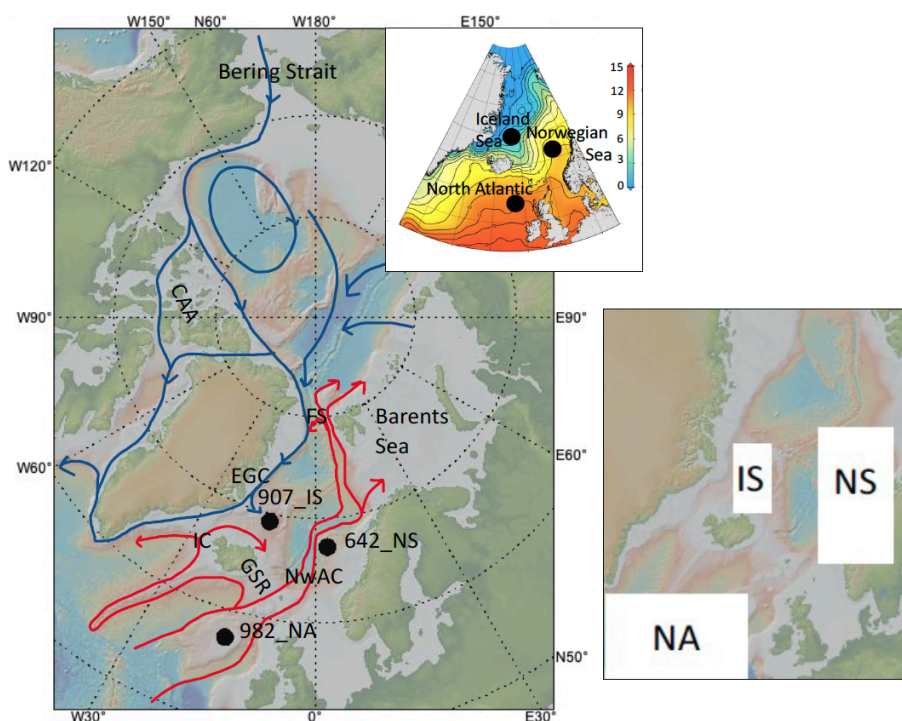
The North Atlantic Current transports warm and saline Atlantic Water northward, through the subpolar North Atlantic and into the Norwegian Sea where the Norwegian Atlantic Current continues the transport towards the Arctic (Fig. 1). A smaller fraction of Atlantic Water also enters the Nordic Seas west of Iceland, through the North Iceland Irminger current. While branches of the Norwegian Atlantic Current are deflected into the Arctic Ocean and the Barents Sea through the



Fram Strait and Barents Sea Opening (Blindheim and Østerhus, 2005; Smedsrud et al., 2022), a large fraction of the Atlantic Water recirculates in the Fram Strait and joins the southward flowing deeper branch of the East Greenland Current (Bourke et al., 1988). Cold fresh water branches off from the East Greenland Current, towards the Iceland Sea.

45 While part of this water re-joins the East Greenland Current, some will continue eastward in the East Icelandic Current and into the Norwegian Sea (Macrandrer et al., 2014). Along its way through the Nordic Seas (i.e. the Norwegian, Greenland and the Iceland Seas) and the Arctic Ocean, the warm and saline Atlantic Water is gradually transformed as it loses heat and gains fresh water (Mauritzen, 1996). At seasonal and interannual time scales, wind forcing is important for the inflow of Atlantic Water across the Greenland Scotland Ridge (Bringedal et al., 2018). However, buoyancy forcing,

50 changing seawater density due to heat (heating/cooling) and/or freshwater (evaporation/precipitation/runoff) fluxes and associated production of dense overflow water that has to be compensated, is key at longer time scales (Furevik et al., 2007; Smedsrud et al., 2022; Talley et al., 2011).



55 **Figure 1** (a) Map of the subpolar North Atlantic, Nordic Seas and Arctic Ocean with a schematic illustration of the main surface currents (currents carrying Atlantic Water are shown in red while currents carrying Polar Water are shown in blue). NwAC: Norwegian Atlantic Current. IC: Irminger Current. EGC: East Greenland Current. FS: Fram Strait. CAA: Canadian Arctic Archipelago. GSR: Greenland Scotland Ridge. 982_NA: Location of ODP Site 982 from the North Atlantic. 642_NS: Location of ODP Site 642 from the Norwegian Sea. 907_IS: Location of ODP Site 907 from the Iceland Sea. (b) The objectively analysed mean regional ocean climatology for 1995 to 2004, represented by annual temperature (°C) at the surface (10 m) using a quarter-degree grid (Seidov et al., 2013; Seidov et al., 2018). Counter interval is 1°C, ranging from 13°C to -1°C. (c) show the domains over which the CMIP6 data are analysed (NA: North Atlantic; NS: Norwegian Sea and IS: Iceland Sea). The same domains are used throughout the paper for conceptual representation of the results, eventually with blue (red) boxes representing cold (warm) SST anomalies (Fig. 6, 8, 9, 10 and 11; Table 1). The figure base is made with GeoMapApp (www.geomapapp.org) / [CC BY](https://creativecommons.org/licenses/by/4.0/) / CC BY (Ryan et al., 2009)).

60



65

The continuous northward transport of heat implies that different sea surface temperature (SST) relationships across the North Atlantic, Norwegian Sea and Iceland Sea may occur at different time scales. Since it takes 3-4 years for SST/heat anomalies to travel from the North Atlantic through the Norwegian Sea (Holliday et al., 2008), out of phase relationships between the seas may exist at interannual-to-decadal time scales. This feature has been documented in observations and Earth System Models (Árthun and Eldevik, 2016; Árthun et al., 2017). Beyond decadal time scales, however, this propagation-driven lag should in theory no longer be of importance, and the default expectation is of an in-phase SST relationship between the North Atlantic, the Norwegian Sea and the Iceland Sea. In other words, it is expected that a warm North Atlantic will entail warm SSTs both in the Norwegian and Iceland Seas. Alternatively, if it is cold in the North Atlantic, the Norwegian and Iceland Seas are also expected to be cold.

75

However, an out of phase relationship between SSTs in the North Atlantic and Norwegian Sea seems to appear even in the context of multidecadal time scales. For example, it emerges in the strongly forced Coupled Model Intercomparison Project (CMIP)5 RCP 8.5 scenario runs for future climate change (Alexander et al., 2018; Nummelin et al., 2017). Alexander et al. (2018) argue that a lack of, or a weaker, warming south of Greenland results from a reduction in the upper ocean poleward heat transport by the Atlantic Meridional Overturning Circulation (AMOC) and lengthened exposure of surface waters to atmospheric heat loss as sinking at high latitudes decreases (Drijfhout et al., 2012; Cheng et al., 2013). Nummelin et al. (2017) and Keil et al. (2020) find that the reduced heat loss from the subpolar North Atlantic furthermore enhances ocean heat transport from the midlatitude North Atlantic to the Arctic. It is suggested that both the overturning and the subpolar gyre circulation contribute to the increased ocean heat transport towards the Norwegian Sea (Keil et al., 2020).

85

These CMIP5 studies (Alexander et al., 2018; Nummelin et al., 2017; Keil et al., 2020) suggest that the expectation of an in-phase SST relation between the North Atlantic, Norwegian and Iceland Seas is not valid under strongly forced, high emission scenarios, and for the associated transient changes expected to take place within the next century. Whether or not the out of phase SST response is restricted to the high emission scenario will be addressed here by comparing those results with a low emission scenario from CMIP. Furthermore, we will investigate SST reconstructions from a past warm climate period with atmospheric CO₂ concentrations comparable to the low emission scenario to explore potential differences in SST responses under equilibrium versus transient forcing. During the Pliocene (5.3 to 2.6 Ma), atmospheric CO₂ concentrations were close to 400 ppm, ranging from 300 to 427 ppm (De La Vega et al., 2020; Bartoli et al., 2011), comparable to the present (ca. 410 ppm) and the future low emission scenarios (Meinshausen et al., 2020; Ippc, 2021). Important to keep in mind is that the long-term background state of Pliocene climate was not forced by an abrupt CO₂ increase, as the future scenarios are. Rather, relatively high CO₂ values existed for millions of years through the Pliocene. The SST phase relations in the North Atlantic, Norwegian and Iceland Seas during the Pliocene may therefore be seen as a realization of equilibrium responses to an atmospheric CO₂ content comparable to today's, in contrast to the transient responses given by the CMIP model scenarios.

100

Here we document existing SST anomalies and phase relations in observational data, CMIP6 Shared Socioeconomic Pathways (SSP)126 experiments and Pliocene alkenone SST reconstruction from the North Atlantic, Norwegian and Iceland Seas. Furthermore, we address why different SST phase relations may emerge and exist across different climate states, time scales and forcing scenarios. Since buoyancy forcing is key for the inflow of Atlantic Water over the Greenland Scotland Ridge (Furevik et al., 2007), we perform a range of idealized sensitivity studies using the

105



Massachusetts Institute of Technology general circulation model (MITgcm) to investigate impacts of changes in buoyancy forcing on the phase relationship between SSTs in the North Atlantic, Norwegian Sea, and Iceland Sea. These idealized experiments provide potential physical explanations on how to set up different SST phase relations. The results of the idealized experiments are furthermore discussed considering reviewed information about known climate characteristics associated with the identified phase relations, to address the likely cause of a specific phase relation taking place. In the discussion we take into account potential impacts on our results of the large temporal and small geographical differences that exist between the observations/future projections and Pliocene reconstructions (Dowsett et al., 2016). By analysing variability across time scales that normally are not seen in context of each other, we provide new perspectives on which spatio-temporal structure of SST patterns may exist under different background climate states and forcing regimes.

2. Data and method

2.1 Observation-based data: HadISST

This data set is from the Met Office Hadley Centre (version 1.1) and provides monthly global SST on a 1-degree latitude-longitude grid over the time period from 1870 to 2012. A detailed description of the dataset is given in (Rayner et al., 2003). In this study we use the annual mean SST to document the existing SST anomalies and their phase relation between the North Atlantic, Norwegian and Iceland Seas. The data is averaged over the following domains: NE North Atlantic (49-57°N, 35-14°W), Norwegian Sea (62.5-73°N, 0-16°E), and Iceland Sea (66-72°N, 18-10°W) (Fig. 1). To investigate multidecadal time scales over the HadISST data set, we apply both a 5-year running mean and a bandpass filter (5-40 years).

2.2 Transient simulations: CMIP6exp ssp126

The current generation of global climate models is available through CMIP6. CMIP6 provides a range of climate change experiments to the end of this century and beyond. Here, we use monthly gridded SST data from the SSP126 experiment covering the time period from 2021 to 2100, with an approximate radiative forcing of 2.6 W/m² and a relatively low level of global warming (it is called the “2°C-scenario”) by 2100. CO₂ concentrations reaches 445ppm by 2100 (Meinshausen et al., 2020), which is at the high end of the Pliocene CO₂ range (Bartoli et al., 2011; De La Vega et al., 2020). Similar to HadISST data, we assess the annual mean SST from each of the model simulations. A 5-year running mean have been used to smoothen interannual variability. Because of the 5-year running mean filter, the time series are shown for the time period 2023 to 2098.

The CMIP6 archive offers model output from many models. In this study, we have chosen to analyse three different models that have different equilibrium climate sensitivity (ECS; Meehl et al., 2020; Seland et al., 2020), leading to different amounts of warming by 2100: CNRM-ESM2-1 having the highest sensitivity of the three models (ECS=4.8), NorESM2-MM the lowest sensitivity (ECS=2.5), and MPI-ESM1-2-LR in between (ECS=3). In the analysis herein, we use one member from each model (i.e., one simulation from each of the three selected models). Some additional model simulations have been included, to check whether the results hold under a more aggressive warming scenario (SSP585 experiment; NorESM2-MM), different resolution in the atmosphere (1 degree versus 2 degrees; NorESM2-MM vs. NorESM2-LM), and more members (10 members compared to one single member; MPI-ESM1-2-LR). The model data is averaged over the following domains: NE North Atlantic (49-57°N, 35-14°W), Norwegian Sea (62.5-73°N, 0-16°E), and Iceland Sea (66-72°N, 18-10°W). SST anomalies relative to the mean of the 5-year running mean filtered time series are calculated for CNRM-ESM-2-1, one of the 10 MPI-ESM1-2-LR members, NorESM2-MM (SSP126) and NorESM2-



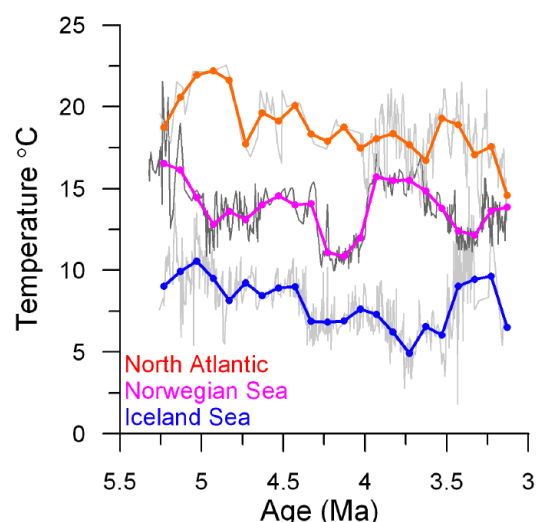
MM (SSP585). We focus on the SST anomalies for the three domains and the relation between these at the end of the century (last three decades).

150

2.3 Pliocene SST reconstructions

To investigate the SST phase relation of the North Atlantic and Nordic Seas during the Pliocene we use a compilation of previously published alkenone $U^{K_{37}}$ SST data from three sites from the northern NE North Atlantic (ODP Site 982; 57.5167°N, 15.8667°W; 1134.2 m water depth) (Herbert et al., 2016; Lawrence et al., 2009), the Norwegian Sea (ODP Site 642; 67.255°N, 2.928333°E; 1280.9 m water depth) (Bachem et al., 2016; Bachem et al., 2017) and the Iceland Sea (ODP Site 907; 69.24815°N, 12.69°W; 1801.5 m water depth) (Herbert et al., 2016) (Fig. 1). Each dataset covers the time interval between 5.23 and 3.13 Ma. All records are presented as previously published (Herbert et al., 2016; Lawrence et al., 2009; Bachem et al., 2016; Bachem et al., 2017), using established age models and the Müller et al. (1998) $U^{K_{37}}$ -SST calibration. The standard error of estimate using this calibration is $\pm 1.5^{\circ}\text{C}$ (Müller et al., 1998). The sampling resolution of the original records varies; for Site 907 (Iceland Sea) the mean original temporal resolution was ca. 2600 years, however, from 3.33 to 3.16 Ma the spacing between measurements ranges from 4000 to 70,000 years; for Site 642 (Norwegian Sea) the mean resolution was ca. 2500 years between 3.13 and 3.49 Ma and ca. 7200 years between 3.49 and 5.23 Ma; and for Site 982 it was ca. 2100 years between 3.13 and 4.03 Ma and ca 40800 years between 4.03 and 5.23 Ma. To enable direct comparison between sites, independent of differences in temporal resolution and absolute ages for the raw data points, each dataset has been resampled every 100 kyr between 5.23 and 3.13 Ma, using a linear integration function in *AnalySeries* (Paillard et al., 1996). The 100-kyr resampling interval is chosen to put focus on the long-term trends of each record and the background climate state upon which the shorter-term orbital variability is superimposed (Fig. 2). The shorter-term orbital variability is not well enough resolved by all records throughout the investigated time interval to allow for a higher resolution resampling. Hence, given the time scales considered here, the phase relations are unlikely to be orbitally forced. Furthermore, focusing on the mean state of longer intervals, rather than point to point comparison, also minimizes the impact of uncertainties from age models which may be on the scale of a few thousands of years.

170



175 **Figure 2** Original $U^{K_{37}}$ SST reconstructions from the North Atlantic, Norwegian and Iceland Seas (grey tones) (Bachem et al., 2016; Bachem et al., 2017; Herbert et al., 2016; Lawrence et al., 2009) with 100 kyr resampled datasets superimposed (North Atlantic (red), Norwegian (magenta) and Iceland Seas (blue)).



2.4 Model set up and reference experiments

180 We use an idealized-topography configuration of the MITgcm (Marshall et al., 1997) to investigate the SST relationships in the study area under a range of forcings (Fig. 1). The set-up (Fig. 3) is a Nordic Seas-like basin separated from a truncated North Atlantic-like source water region by a 1000 m deep ridge. Both basins are flat-bottomed with 2000 m depth and surrounded by sloping sides. The model domain is closed. The boundary conditions and prescribed forcings are the following: There is a restoring boundary condition in the south maintaining the reservoir of Atlantic source water
185 (of temperature $T_A = 6^\circ\text{C}$ and salinity 35 psu). In addition, SSTs are restored toward atmospheric temperatures (SAT) through the surface heat flux which is parameterized as " $Q=(\text{SST}-\text{SAT})*G$ " where $G=40\text{W}/\text{m}^2\text{C}$. There is no interactive atmosphere. There is a constant uniform precipitation north of the ridge. Mechanical forcing is provided by a constant-in-time prescribed wind field (W) with westerlies over the North Atlantic and easterlies over the Nordic Seas field. The latitude of zero wind-stress curl is in the middle of the Atlantic region, with cyclonic wind stress to the north and anti-cyclonic to the south.
190

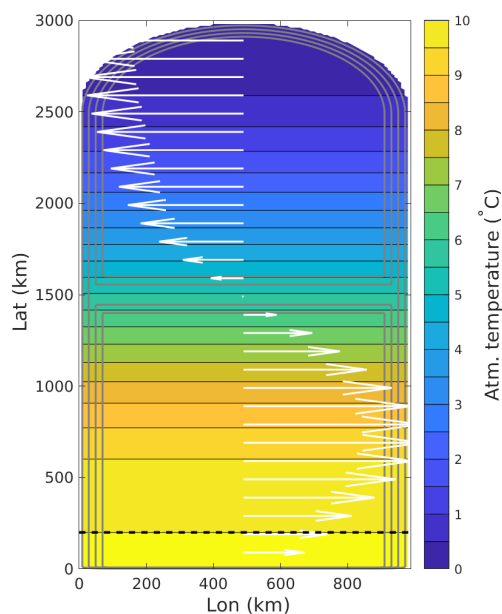
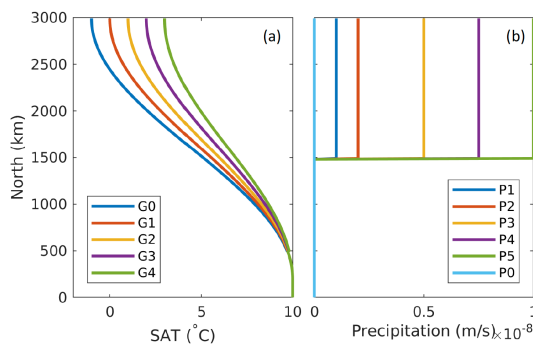


Figure 3 The model setup. Grey contours outline the bathymetry (every 300 m), colours show the SAT (profile G1 in Fig. 4), and white arrows represent the wind forcing. Fig. 4 provides an overview of the different SAT and precipitation forcing used for the experiments. South of the black dashed line salinity is restored to 35 psu and oceanic temperature is restored to 6°C .
195

The horizontal resolution is 10 km and there are 30 vertical layers; the upper 20 layers are 50 m thick and the deepest layers are 100 m thick. Water density is calculated using the formula from Jackett and McDougall (1995), with a constant Coriolis parameter, $f=1.2*10^{-4}\text{s}^{-1}$, and vertical diffusivity and viscosity of $1*10^{-5}\text{m}^2\text{s}^{-1}$. Convection is parameterized with implicit vertical diffusion; the diffusivity increases to $1000\text{m}^2\text{s}^{-1}$ for statically unstable conditions. Horizontal viscosity is parameterized using the Smagorinsky closure (Smagorinsky, 1963): Typical values are $30\text{m}^2\text{s}^{-1}$ for the boundary current region. Temperature and salinity are advected using a third-order flux-limiting scheme.
200



205 Since one of the key drivers for inflow of Atlantic Water to the Norwegian Sea is buoyancy forcing and production of dense overflow water that has to be compensated (Furevik et al., 2007), we change the SAT (G) and the precipitation (P) north of the ridge to study the impact of buoyancy forcing on the phase relationships between SSTs in the North Atlantic, Norwegian Sea, and Iceland Sea. The SAT and precipitation are changed as shown in Fig. 4. Note that the SAT over the restoring region is the same for all experiments. We define three reference experiments, REF-1 (G0 and P1), REF-2 (G1 and P1) and REF-3 (G0 and P3). REF-1 is set up to investigate the oceanographic responses to a gradually decreasing SAT gradient between the North Atlantic and the Nordic Seas, by increasing the SATs over the Nordic Seas. For the REF-2 experiments, the buoyancy is changed by gradually increasing the precipitation over the Nordic Seas while SAT is kept constant. The REF-3 experiments are similar to the REF-1 experiments in the sense that SAT over the Nordic Seas are increased, however, the initial state of the Nordic Seas is fresher for REF-3 than for REF-1. Hence the REF-3 experiments are set up to see how the initial state of the ocean may impact the responses to increased SAT over the Nordic Seas. The idealized model is run for 30 years, to near steady-state, and we present results from the last 5 years of the runs which are compared to the results from the relevant reference experiment. We are therefore not studying transient changes, but differences between equilibrium states.



220 **Figure 4** (a) SAT forcing and (b) precipitation forcing for experiments.

The combination of the prescribed wind stress and the steep yet sloping coastal boundary supports a cyclonic boundary-intensified circulation around the Nordic Seas. The reference experiments have an ocean circulation which represents the main characteristics of the North Atlantic (south of the ridge), with an anticyclonic gyre in the “subpolar” latitudes and a cyclonic gyre further south. The buoyancy forcing from the prescribed surface temperature and salinity results in a gradual meridional temperature decrease and similar salinity decrease mimicking northern heat loss and freshwater input (Fig. 5). The thermal forcing dominates, and there is net northern buoyancy loss. There is warm and saline inflow to the Nordic Seas-like basin, and a colder and fresher outflow. The densest and coldest water is found in the relatively motionless and weakly stratified interior of the Nordic Seas. The overall temperature contrast between the dense-water interior and the Atlantic source water region reflects the temperature range of the prescribed surface air temperature. Waters are continuously exchanged between the buoyant boundary current and the interior by lateral eddy-mixing. Heat is thus not only lost from the boundary current by air-sea interaction but also by lateral heat loss to the interior, where it is also given up to the atmosphere.

235 When presenting MITgcm results, the North Atlantic domain is defined as the North Atlantic restoring region (Fig. 5c), set to be 6°C for all experiments (Fig. 4a). The Norwegian Sea domain is defined as a box in the eastern boundary current



region, while the Iceland Sea domain is represented by the interior ocean north of the ridge (Fig. 5c). These boxes are set to represent similar areas as those introduced in sec 2.2. We identify SST phase relationships between these three regions by comparing the temperature of the sensitivity experiment with the relevant reference experiment. A significant temperature change in one region is defined as a temperature change where the change between two experiments exceeds $2\sigma(\text{SST}_{\text{reference_experiment}})$. As the North Atlantic is set to constant, this is never the case for this region. Thus, a change in phase relationship between the three regions exists if there is a significant temperature change in either the Norwegian Sea or the Iceland Sea, or both.

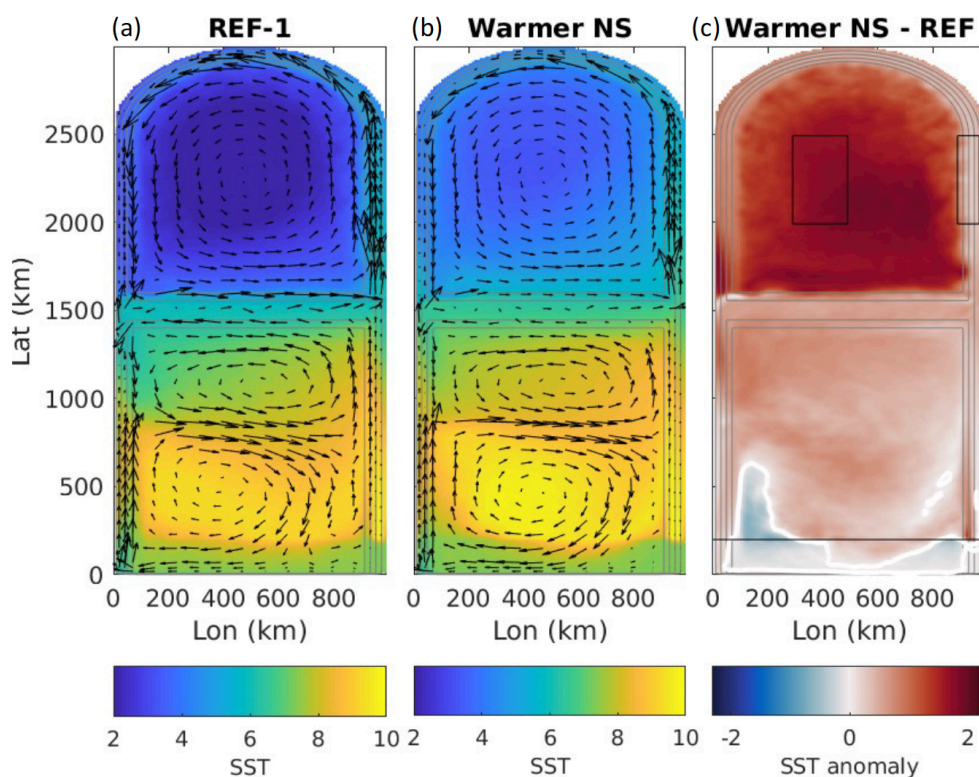


Figure 5 SSTs (colours) and upper 500 m ocean circulation (black arrows) for experiments (a) REF-1 and (b) Warmer NS (G3, P1). (c) shows the difference between the two experiments. White mark the zero-contour line, and boxes show the areas used to calculate the SSTs of the Norwegian Sea (pink) and the Iceland Sea (blue) used in Table 1. The North Atlantic restoring region equals the area south of the red line in (c).

250

3 Results

First, the phase relations between SST anomalies in the North Atlantic, Norwegian and Iceland Seas, as seen in HadISST (multidecadal time scales), the low-emission future scenario runs (CMIP6 SSP126; multidecadal time scale) and Pliocene SST reconstructions (over several 100 kyr) are presented. Thereafter, we present the results of the idealized experiments testing the impact of changes in buoyancy forcing.

255

3.1 Phase relations in observation-based data: HadISST



The annual SST anomalies on interannual-to-decadal time scales, as seen in the HadISST dataset, vary between -0.8 and +0.8°C (Fig. 6). As expected at these time-scales (Årthun and Eldevik, 2016; Årthun et al., 2017), we find antiphase (Norwegian Sea/NE North Atlantic) and in-phase relationships (Norwegian Sea/Iceland), with significant correlations for bandpass filtered time series (Fig. 7). However, as described in the introduction, on multidecadal time scales this antiphase should in theory no longer be of importance, and we see an in-phase SST relationship between the North Atlantic, the Norwegian Sea and the Iceland Sea (Fig. 6). On multidecadal time scales, these regions follow to a large extent the Atlantic Multidecadal Variability (AMV), with a warm phase in 1930-1970 and a cold phase in 1970-1990 (Knight et al., 2005).

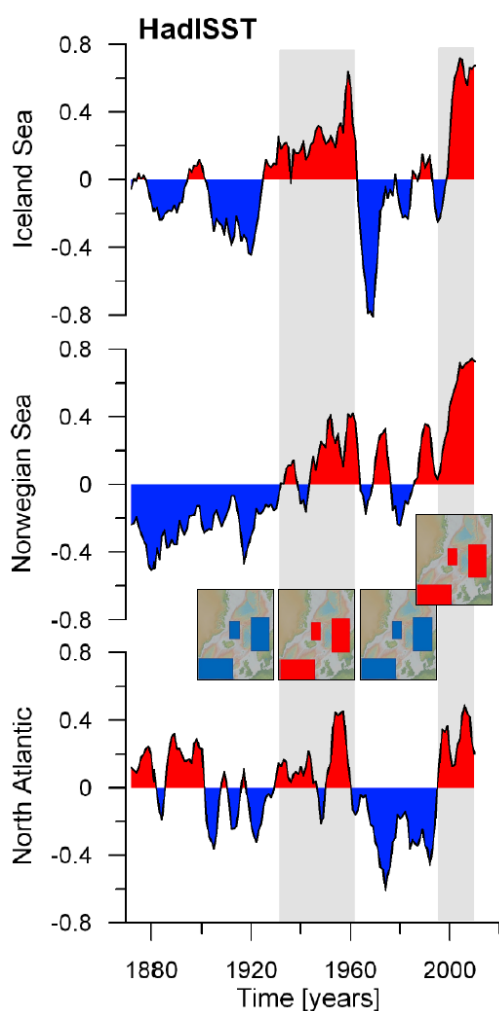
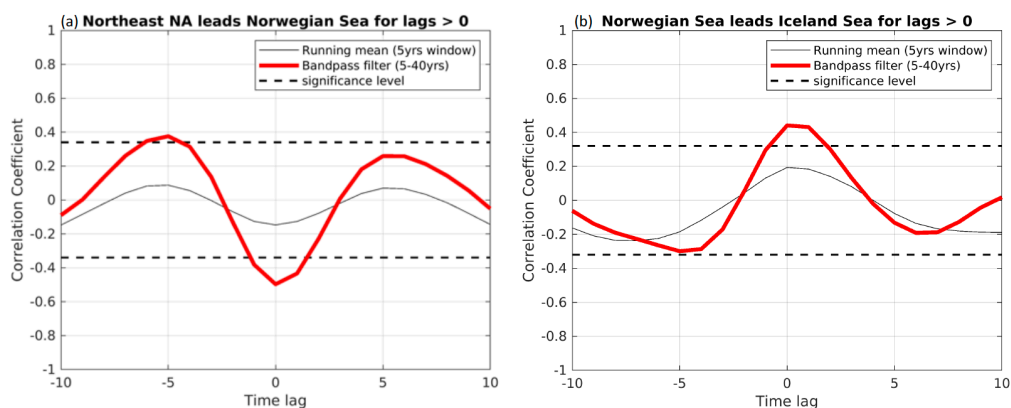


Figure 6 Annual SST anomalies for the North Atlantic, Norwegian and Iceland Seas based on HadISST data. SST have been averaged over the three box regions before calculating the anomalies: 49-57°N and 14-35°W (North Atlantic), 62.5-73°N and 0-16°E (Norwegian Sea), 66-72°N and 10-18°W (Iceland Sea). A running mean with a 5-year window has been applied on the time series and the anomalies are shown relative to the mean of the 5-year running mean filtered time series (2023-2098). The map inserts provide a conceptual representation of the results, with blue (red) boxes representing cold (warm) SST anomalies for the North Atlantic, Norwegian and Iceland Seas. The base for the map inserts is made with GeoMapApp (www.geomapp.org) / [CC BY](https://creativecommons.org/licenses/by/4.0/) / CC BY (Ryan et al., 2009)).



275

Figure 7 (a) Correlations at different time lags (in years) between the North Atlantic and Norwegian Sea. (b) Correlations at different time lags between the Norwegian Sea and Iceland Sea. Significant correlations at the 95% level (black dashed line) by the standard two-sided Student's t-test and considering autocorrelation. Correlations have been calculated both by applying a 5-year running mean and a bandpass filter (5-40 years) on the time series. Note that these correlations are calculated using the winter values (Jan-Apr) over the period 1870-2012, as the propagation is most evident during wintertime (Årthun et al., 2017).

280

3.2 Future phase relations - CMIP6exp: ssp126

The three models, CNRM-ESM2-1, MPI-ESM1-2-LR and NorESM2-MM, show different results, both with respect to their SST climatology and the SST anomalies in each region of interest over the later part of the 21st century (Fig. 8). The mean SST of the 5-year running mean filtered time series (2023-2098) of the NE North Atlantic is fairly similar in the three models, but the Norwegian Sea differs to some extent with MPI-ESM1-2-LR being warmest (9.5°C), NorESM2-MM being coldest (6.8°C), and CNRM-ESM2-1 in between (7.8°C). The mean SST in the Iceland Sea differs to a large extent among the three models, again with MPI-ESM1-2-LR being warmest (5.6°C) and NorESM2-MM coldest (0°C).

285

CNRM-ESM2-1 shows larger SST anomalies for the Norwegian Sea and the Iceland Sea than the two other models (Fig. 8b). This is consistent with CNRM-ESM2-1 being the most sensitive, or more rapidly responding, model (as described in Section 2.2). Based on CNRM-ESM2-1, we find a dominantly cold SST anomaly in the North Atlantic and a warm SST anomaly in the Norwegian and the Iceland Seas towards the end of the 21st century. Thus, for the SSP126 scenario CNRM-ESM2-1 suggests that the North Atlantic will be out of phase with the Norwegian and Iceland Seas at the end of the 21st century (2068-2098).

290

295

In contrast to the CNRM-ESM2-1 results, MPI-ESM1-2-LR and NorESM2-MM show much smaller SST anomalies at the end of the 21st century, relative to the models mean SST over the next century, for the North Atlantic, Norwegian and Iceland Seas for the SSP126 scenario (Fig. 8b). Considering 10 different members from MPI-ESM1-2-LR, we find that the results from the individual members do not differ to a large extent (Fig. 8a); neither of the members show anything but minor SST variability and the difference between the members is less than the amplitude of the changes in CNRM-ESM2-1. On the other hand, considering a more aggressive scenario (SSP585) for NorESM2-MM, we find a clear warm anomaly in the Norwegian and the Iceland Seas (Fig. 8b). A cold, but small, SST anomaly is seen for the North Atlantic. Furthermore, we find that lowering the horizontal resolution in the atmosphere enhances the SST in the Iceland Sea but lowering the resolution does not have a clear effect on the SSTs of the two other regions (Fig. 8a).

300

305

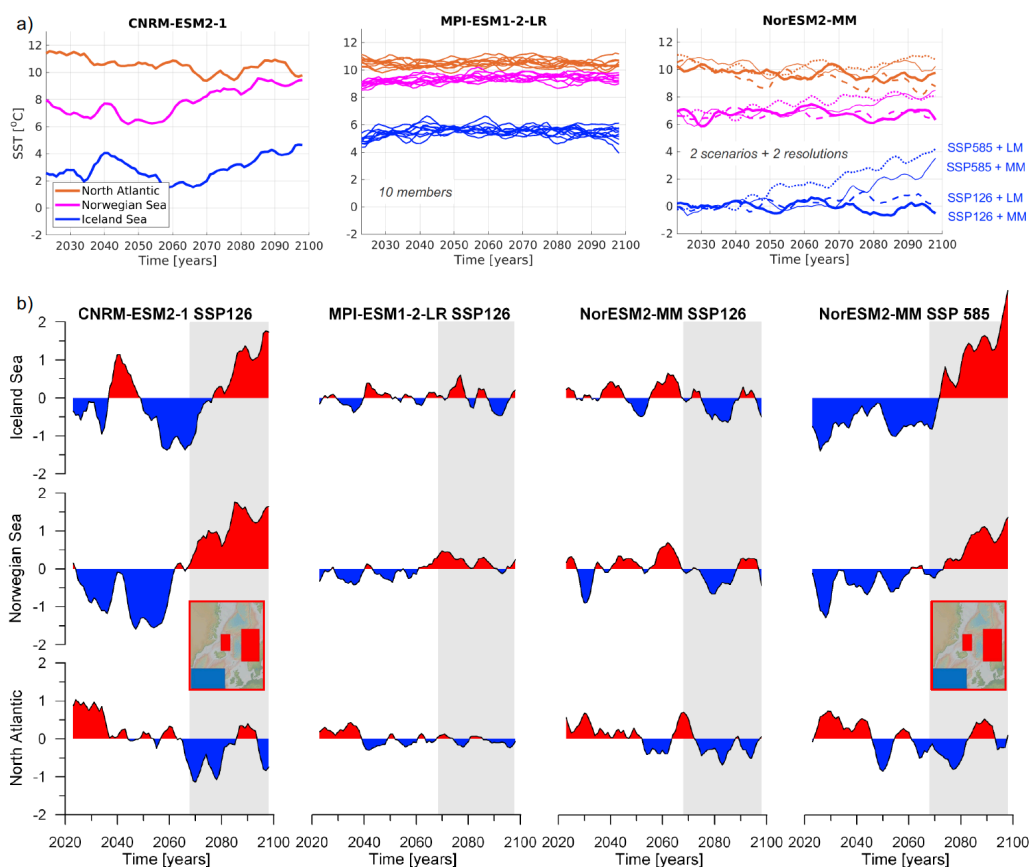


Figure 8 a) Annual mean SST based on CMIP6 future scenario SSP126, representing the North Atlantic (red), Norwegian (magenta) and Iceland Seas (blue). SST have been averaged over the same box regions as described in Fig. 3. CNRM-ESM2-1 displays one member, MPI-ESM2-2-LR displays 10 members, and NorESM2-MM displays two different scenarios (SSP126/thick curves and SSP585/thin curves) and two different atmospheric resolutions (medium/solid curves and low/dashed curves). A running mean with a 5-year window has been applied on the time series. b) SST anomalies relative to the mean of the 5-year running mean filtered time series (2023 to 2098) from CNRM-ESM2-1 (SSP126), one of the 10 MPI-ESM1-2-LR members, NorESM2-MM (SSP126) and NorESM2-MM (SSP585). We focus on the SST anomalies for the three domains and the relation between these at the end of the century (last three decades, marked by the grey bars). The map inserts provide a conceptual representation of the results, with blue (red) boxes representing cold (warm) SST anomalies for the North Atlantic, Norwegian and Iceland Seas. The base for the map inserts is made with GeoMapApp (www.geomapapp.org/) / [CC BY](https://creativecommons.org/licenses/by/4.0/) / CC BY (Ryan et al., 2009).

3.3 Phase relations in Pliocene SST reconstructions

The phase relation between the North Atlantic, Norwegian Sea and Iceland Sea SST anomalies are not constant through the Pliocene. Two different out of phase SST relations are documented: 1) The Norwegian Sea being out of phase with the North Atlantic and the Iceland Sea, either with a warm Norwegian Sea anomaly corresponding with a cold anomaly in the North Atlantic and Iceland Sea (first yellow period in Fig. 9; 3.63-3.93 Ma), or the opposite, a cold anomaly in the Norwegian Sea corresponds to a warm anomaly in the North Atlantic and Iceland Sea (second yellow period in Fig. 9; 4.73-4.93 Ma). 2) A cold anomaly in the North Atlantic and the Norwegian Sea corresponds to a warm anomaly in the Iceland Sea (blue time period in Fig. 9; 3.23-3.43 Ma). All these Pliocene SST phase relationships are different from the



phase relation found in the CMIP6 future runs (warm Norwegian Sea and Iceland Sea, cold North Atlantic). In addition to the out of phase SST relations, there are three time periods during the Pliocene that show an in-phase relationship, comparable to what we find for the observation-based data (grey time periods in Fig. 9; 4.03-4.33 Ma, 4.43-4.63 Ma and 5.03-5.23 Ma).
330

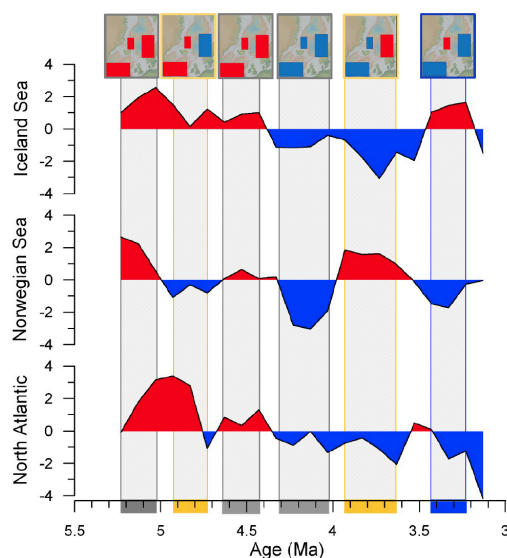


Figure 9 Pliocene SST anomalies (°C, relative to the mean of the 100 kyr resampled records). The different phase relations identified is colour coded (grey boxes - all regions in-phase; blue box - Iceland Sea out of phase with North Atlantic and the Norwegian Sea; yellow boxes - the Norwegian Sea out of phase with the North Atlantic and the Iceland Sea). Conceptual illustrations of the respective phase relations for each interval are shown for all identified scenarios, with blue (red) boxes representing cold (warm) SST anomalies for the North Atlantic, Norwegian and Iceland Seas (from left to right: positive in-phase; cold Norwegian Sea, warm North Atlantic and Iceland Sea; positive in-phase; negative in-phase; warm Norwegian Sea, cold North Atlantic and Iceland Sea; and warm Iceland Sea, cold North Atlantic and Norwegian Sea). The base for the map inserts is made with GeoMapApp (www.geomapapp.org/) / [CC BY](https://creativecommons.org/licenses/by/4.0/) / CC BY (Ryan et al., 2009).
335
340

3.4 Buoyancy forced phase relationships - results from the MITgem idealized experiments

By changing the buoyancy forcing as shown in Fig. 4 and 5 we can produce three different phase relationships in the idealized model: all three regions in-phase (grey experiments, Table 1 and Fig. 10b); Norwegian Sea and Iceland Sea out of phase with North Atlantic (red experiments, Table 1 and Fig. 10); and Iceland Sea out of phase with North Atlantic and the Norwegian Sea (blue experiments, Table 1 and Fig. 10). Hence, these idealized experiments can capture two of the three phase relations found during the Pliocene (grey and blue time periods in Fig. 9) and the phase relationship found in the CMIP6 future runs (Fig. 8). Table 1 summarizes the experiments. The first set of four experiments have the same precipitation (P1), but a decreasing SAT-gradient (i.e., increasing SAT over the Nordic Seas (G1-G4)) relative to REF-1. As SAT increases over the Nordic Seas the SST pattern shift from the Iceland Sea being out of phase with the North Atlantic and the Norwegian Sea (G1) to the North Atlantic out of phase with the Norwegian and Iceland Seas (G2-G4) (Fig. 10a). In the next set of experiments SAT is kept constant (G1) while the precipitation over the Nordic Seas is increased (P2-P5) relative to REF-2. With increasing precipitation over the Nordic Seas, the SST pattern transfers from in phase (insignificant responses; P2 and P3) to the Iceland Sea being out of phase with the North Atlantic and the Norwegian Sea (P4) to the North Atlantic out of phase with the Norwegian and Iceland Seas (P5) (Fig. 10b). In the last
345
355



set of experiments, the decreasing SAT-gradient experiments (G1-G2) are repeated with a fresher Nordic Seas (P3) relative to REF-3. As for REF-1, the SST pattern shift from the Iceland Sea being out of phase with the North Atlantic and the Norwegian Sea (G1) to the North Atlantic out of phase with the Norwegian and Iceland Seas (G2) when we increase the SAT over the Nordic Seas (Fig. 10c).

360

Table 1 Selected output from the MITgcm idealized model experiments. SAT is atmospheric temperature forcing (Fig. 4), Prec is precipitation forcing (Fig. 4), T_{nws} and T_{ice} is sea surface temperature of the boundary current/Norwegian Sea and interior/Iceland Sea (Fig. 5) for the three reference experiments. $\Delta T_{nws-ref}$ and $\Delta T_{ice-ref}$ is the temperature difference between the experiment and the corresponding ref-experiment for the boundary current/Norwegian Sea and interior/Iceland Sea, respectively. The numbers are marked in bold if the temperature difference exceeds the 2*std of the reference experiment. $\Delta D_{north-south}$ is the density difference between north (averaged over 2000-2500 km) and south (averaged over 500-1000 km) of the ridge within each experiment over the full depth. V_{inflow} is the mean inflow velocity across the sill (cm/s) (at 1500 km), V_{bc} is the mean velocity in the boundary current (cm/s) (average for the Norwegian Sea as defined by the pink box in Fig. 5), HT_{sill} is the net heat transport across the sill (TW) (at 1500 km), and NMOC (Sv) is the maximum overturning streamfunction at the sill (at 1500 km). Ref-exp is the corresponding reference experiment which the experiment is compared against. The three different phase relations identified is colour coded (grey - all regions in-phase; red - Norwegian Sea and Iceland Sea out of phase with North Atlantic; blue - a significant change in the Iceland Sea and no change in the Norwegian Sea and North Atlantic, considered to be a representation of Iceland Sea out of phase with North Atlantic and the Norwegian Sea).

365

370

Exp / Colour code	SAT	Prec	$T_{nws} \pm 2std(T_{nws})$	$T_{ice} \pm 2std(T_{ice})$	$\Delta T_{nws-ref}$	$\Delta T_{ice-ref}$	$\Delta D_{north-south}$	V_{inflow}	V_{bc}	HT_{sill}	NMOC (Sv)	Ref-exp
REF-1	G0	P1	5.18±0.16	1.71±0.15			0.36	1.76	10.92	100.59	3.72	
Warmer NS / blue	G1	P1			0.10	0.51	0.33	1.62	9.95	82.33	3.33	REF-1
Warmer NS / red	G2	P1			0.28	1.11	0.30	1.44	8.76	59.24	2.89	REF-1
Warmer NS / red	G3	P1			0.44	1.74	0.25	1.54	7.19	39.24	2.49	REF-1
Warmer NS / red	G4	P1			0.69	2.42	0.2	1.05	5.58	24.57	1.99	REF-1
REF-2	G1	P1	5.28±0.11	2.22±0.10			0.33	1.62	9.95	82.33	3.33	
Fresher NS / grey	G1	P2			0.02	0.00	0.32	1.59	9.67	82.25	3.34	REF-2
Fresher NS / grey	G1	P3			-0.04	-0.08	0.31	1.45	8.94	76.78	3.26	REF-2
Fresher NS / blue	G1	P4			-0.05	-0.54	0.27	1.82	7.34	70.66	3.42	REF-2
Fresher NS / red	G1	P5			-0.17	-0.64	0.23	1.66	5.86	59.52	2.86	REF-2
Saltier NS / grey	G1	P0			0.04	0.07	0.33	1.47	10.10	82.17	3.24	REF-2
REF-3	G0	P3	5.16±0.12	1.61±0.09			0.34	2.00	10.34	94.21	3.64	
Warmer NS / blue	G1	P3			0.08	0.53	0.31	1.45	8.94	76.78	3.26	REF-3
Warmer NS / red	G2	P3			0.25	0.96	0.26	1.41	7.44	54.50	2.88	REF-3

375

Reducing the SAT-gradient, i.e., warming the atmosphere over the Nordic Seas, reduces the heat loss from the ocean and warms the SSTs in the Nordic Seas. Compared to the reference experiment, the following are smaller: the north-south density difference; the mean inflow velocity across the ridge; the boundary current velocity in the Nordic Seas; the net heat transport across the sill; the maximum overturning circulation across the sill; and the lateral eddy heat transport in the Nordic Seas (Table 1). The changing ocean circulation transports less heat to the Norwegian Sea/Nordic Seas. In

380



addition, as the boundary current in the Nordic Seas is slower in warmer experiments, the water experiences more cooling as it travels the Nordic Seas, allowing for a larger heat loss in the Norwegian Sea region.

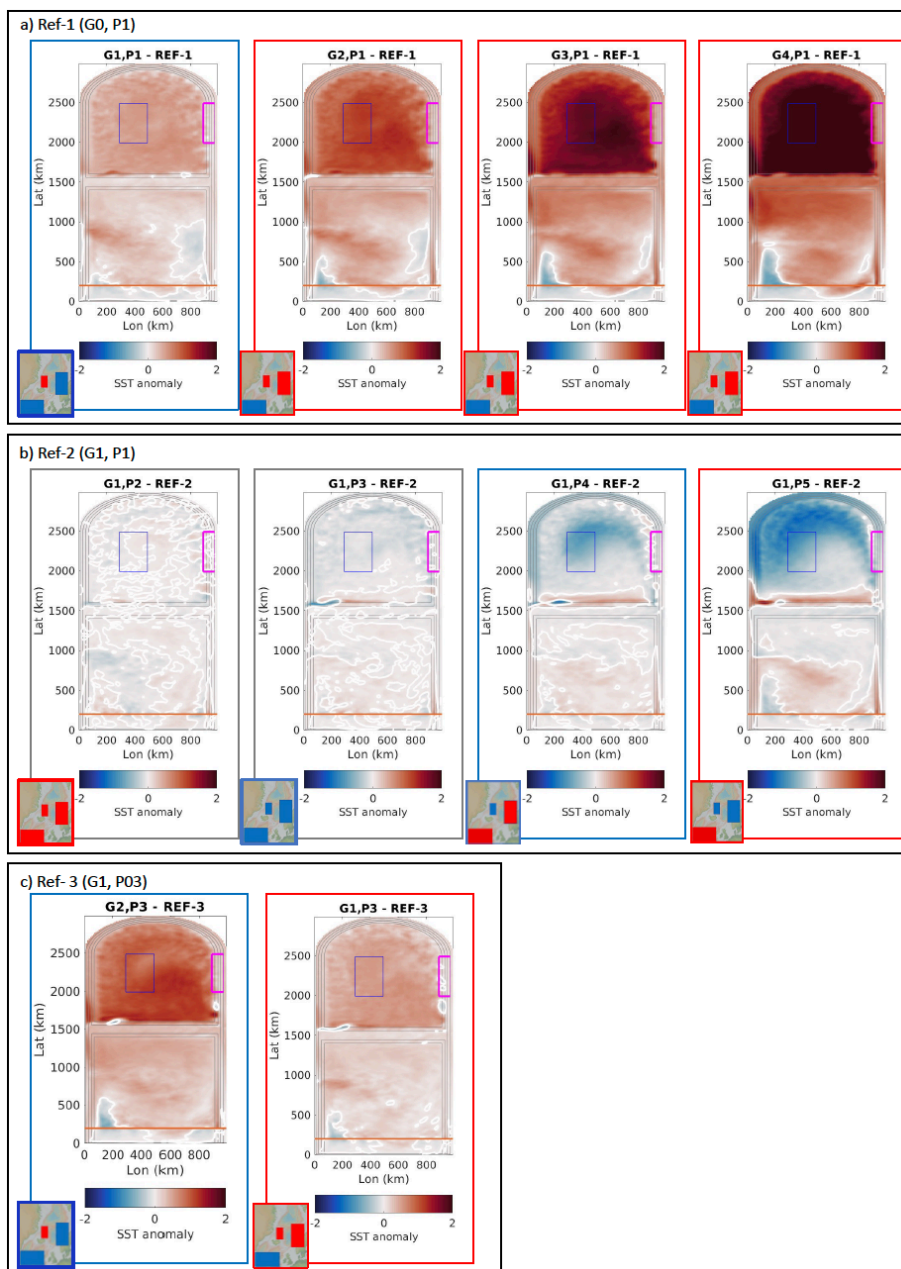


Figure 10 SST anomalies seen in MITgcm idealized experiments. Surrounding blue boxes represent Iceland Sea out of phase with the North Atlantic and the Norwegian Sea. Surrounding red boxes represent North Atlantic out of phase with the Norwegian and Iceland Seas. Surrounding grey boxes represent in phase between the three regions (not significant responses). Conceptualized representation of the resulting phase relations is shown by the map inserts, where blue (red) boxes represent cold (warm) SST anomalies for the North Atlantic, Norwegian Sea and Iceland Sea. The base for the map inserts is made with GeoMapApp



(www.geomapapp.org) / [CC BY](#) / CC BY (Ryan et al., 2009)). a) SST anomalies relative to reference experiment 1, where precipitation is kept constant at P1 while SAT is gradually increased (G1-G4). b) SST anomalies relative to reference experiment 2, where SAT is kept constant at G1 while precipitation is gradually increased (P2-P5). c) SST anomalies relative to reference experiment 3, where precipitation is kept constant at P3 while SAT is increased (G1 and G2).

385 For the experiments with a small atmospheric forcing change (G1 relative to REF-1 and G1 relative to REF-3; blue experiments in Table 1 and Fig. 10a and c), the increased heat loss and decreased poleward heat transport are partly able to compensate for the increased atmospheric warming in the Norwegian Sea, and thus there is no significant temperature change in the Norwegian Sea. However, this is not the case for the Iceland Sea where the SSTs increase. We consider this result, as representative for an Iceland Sea out of phase with the Norwegian (and Atlantic) Sea, setting up an SST field
390 that breaks the expected SST field of the region. However, we do acknowledge that strictly speaking this is not an anti-phase since the Norwegian Sea (and the North Atlantic) does not cool.

For larger changes in atmospheric forcing (G2-G4 relative to REF-1 and G2 relative to REF3; red experiments; Table 1 and Fig. 10a and c), both the Iceland and Norwegian Sea experience a significant temperature increase. There is a larger
395 temperature change in the Iceland Sea than in the Norwegian Sea and the difference increases with weaker SAT-gradients. Thus, the absolute temperature for the Iceland Sea is more like the Norwegian Sea for a warmer atmosphere over the Nordic Seas. The larger SST change in the Iceland Sea can be explained by a combination of reduced heat transport to the Norwegian Sea/Nordic Seas and slower Nordic Seas boundary current allowing for a larger heat loss in the Norwegian Sea region and more cooling of the water as it travels the Nordic Seas. The increased heat loss and decreased poleward
400 heat transport counteracts the general atmospheric warming over the Norwegian Sea more so than over the Iceland Sea.

Increasing the north-south salinity gradient across the sill (REF-2 experiments) gives similar results; no significant SST-change in the two regions for small changes in forcing (P2-P3 relative to REF2), an SST change only in the Iceland Sea for medium changes in forcing (P4 to REF-2), and SST changes in both the Iceland and Norwegian Seas for the largest
405 changes in forcing (P5 to REF-2, equal to a precipitation increase from 1 to $10 \cdot 10^{-9}$ m/s (Fig. 4)) (Table 1 and Fig. 10b). A fresher Nordic Seas weakens the north-south density gradient which weakens the poleward heat transport and the boundary current velocity. The slower boundary current allows for more heat loss to the atmosphere in the Norwegian Sea, and the region cools. In these experiments, there is no prescribed warming of the atmosphere, so temperature change is only set by the changes in ocean circulation. The slower boundary current also reduces the eddy heat fluxes from the
410 boundary to the interior, and hence also the Iceland Sea region cools.

Within the investigated parameter space, we have not found a situation where the increased heat loss and decreased poleward heat transport more than compensates for the increased atmospheric warming so that the Norwegian Sea temperature change is opposite to that of the other two regions (i.e., the situation seen for the yellow time periods in Fig.
415 9).

We have limited our study to the impact of buoyancy forcing on SST relationships. Using a similar model configuration, Spall (2011) and Spall (2012) report on the impact of changing sill depth on the temperature of the interior region (the inflowing temperature, i.e., Norwegian Sea temperature is assumed to equal that of the source region). A deeper sill
420 increases the temperature of both the boundary current and the interior of the Nordic Seas. The difference in temperature



between these two regions decreases for larger sill depths. The changes are associated with a strengthening of the meridional overturning circulation across the sill, and to a lesser extent to an increase in heat transport across the sill.

4 Discussion

425 In this study, we have identified four different SST phase relations (Fig. 11): 1) The North Atlantic, Norwegian and Iceland Seas SST anomalies being in-phase (at multidecadal time scales in the observation-based records and over hundreds of thousands of years for three Pliocene intervals (4.03-4.33 Ma, 4.43-4.63 Ma and 5.03-5.23 Ma; Fig. 6 and 9). 2) The Iceland Sea being out of phase with the North Atlantic and the Norwegian Sea (over two hundred thousand years in the Pliocene, 3.23-3.43 Ma; Fig. 9). 3) The North Atlantic being out of phase with the Norwegian and Iceland Seas (at multidecadal time scales in the future, Fig. 8). 4) The Norwegian Sea being out of phase with the North Atlantic and the Iceland Sea (again over hundreds of thousands of years during the Pliocene, 3.63-3.93 Ma and 4.73-4.93 Ma; Fig. 9). From our idealized MITgcm experiments for the North-Atlantic - Nordic Seas region, three of the four different phase relations (1, 2 and 3) could be reproduced by changing the buoyancy forcing (atmospheric temperature and precipitation, Table 1; Fig. 10; Fig. 11).

435

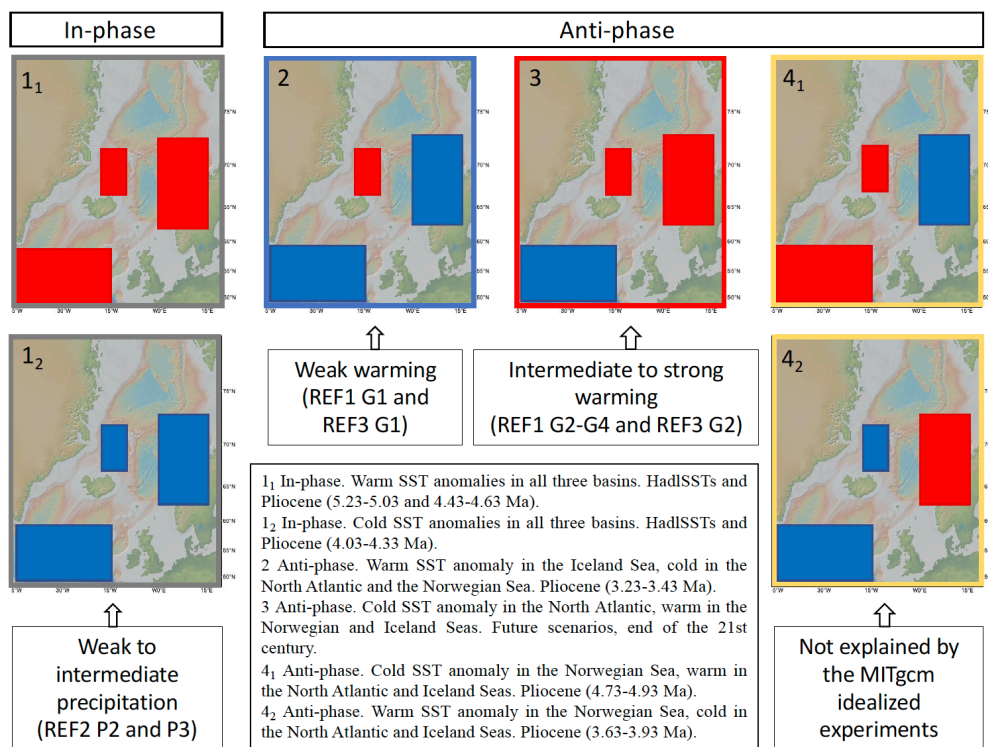


Figure 11 Conceptual illustration of the identified phase relations, showing for which period the explicit phase relations are seen and which MITgcm idealized experiment resulted in the same type of SST relationships. Blue (red) boxes representing cold (warm) SST anomalies. The background maps are made with GeoMapApp (www.geomapapp.org) / [CC BY](https://creativecommons.org/licenses/by/4.0/) / CC BY (Ryan et al., 2009).

We provide a review of global SSTs, overturning circulation and ventilation of the Nordic Seas, tropical SST changes, the Atlantic Ocean equator-pole SST gradient, freshwater and wind forcing to characterize the background states for the identified phase relations seen in the Pliocene and future scenarios (Table 2). The content of Table 2 will, together with



440 Table 1, form the basis for the discussion. For some parts of the Pliocene interval, some of these factors are not thought to have changed (e.g., tropical SSTs), or to our knowledge it is not known what changes may have taken place (e.g., winds); these are not considered further through the discussion.

445 **Table 2** An overview of reviewed information with respect to the Atlantic Ocean equator-pole SST gradient, ocean circulation changes (AMOC, relative proportion of North Atlantic Deep Water (NADW) and ventilation of the Nordic Seas), global SSTs, tropical SSTs, freshwater, wind, and temperature over Norway, for the Pliocene and future. Pliocene information is extracted from available published reconstructions, after resampling every 100 kyr and in most cases presented as anomalies relative to the Pliocene resampled mean, hence, in the exact same manner as for the North Atlantic, Norwegian and Iceland Seas SST datasets analysed (Section 2.1), to secure methodological consistence on how information is extracted (further information and figures showing the relevant resampled datasets as anomaly plots are available in the Supplementary Information). All information related to future is based on a literature review. The different phase relations identified is given a colour code that reflects the colour code used throughout the paper (grey - all regions in-phase; blue - Iceland Sea out of phase with North Atlantic and the Norwegian Sea; yellow - the Norwegian Sea out of phase with the North Atlantic and the Iceland Sea; red - the North Atlantic out of phase with the Norwegian and Iceland Seas).

Time interval	5.03-5.23 Ma	4.73-4.93 Ma	4.43-4.63 Ma	4.03-4.33 Ma	3.63-3.93 Ma	3.23-3.43 Ma	CMIP6 (future trend)
SST phase relation	Positive in-phase (grey)	Cold NS, warm NA and IS (yellow)	Positive in-phase (grey)	Negative in-phase (grey)	Warm NS, cold NA and IS (yellow)	Warm IS, cold NA and NS (blue)	Cold NA, warm NS and IS (red)
Atlantic equator-pole T°C gradient ¹	Overall weaker than WOA _{Annual mean 0-20 m} (Locarini et al., 2018).						
AMOC/%NADW ²	Strong (91)	Strong (69)	Strong (79)	No change (66)	No change (64)	Weak (23)	Weak in all scenarios (Weijer et al., 2020).
Nordic Seas deep ventilation ³	No deep ventilation in the Nordic Seas (Jansen et al., 2000; Risebrobakken et al., 2016).						No indication of reduced deep-water formation (Furevik et al., 2002 [^]).
Norwegian Sea Ventilation, intermediate depth ⁴	Weak	Weak	Weak	No change	Strong	Strong	
Norwegian Sea ventilation, upper water column ⁴	Weak	Strong	Strong-to-weak	Weak	Strong	Strong	
Global SSTs ⁵	Overall higher SSTs relative to today; weaker meridional gradients. Most sites experience cooling through the Pliocene, hence, moving from more positive to more negative anomalies relative to mean of self.						Overall higher SST, except the subpolar North Atlantic in SSP126 (Kwiatkowski et al., 2020).
Tropical change ⁶	Overall warmer than today by approximately 2°C (26.7(+0.2/-0.3)°C _{Pliocene} vs 24.4°C _{WOA Annual mean 0-20m}).						Overall warmer than today by approximately 0-2°C in SSP126 (Kwiatkowski et al., 2020).
	*	*	26.7°C	26.9°C	26.9°C	26.4°C	
Freshwater/Salinity ⁷	No trace of sea ice. Extent unknown.		IS: Indication of sea ice from 4.5 Ma	Traces of sea ice in the Iceland Sea and at the Yermak Plateau (maximum extent as for present summers)			No sea ice in the IS in September, but could be some in March in SSP126 (Wei et al., 2020; Derepentigny et al., 2020)
	-	-	-/+	+	++	++	
	Closed Bering Str./closed CAA: less liquid freshwater into the Nordic Seas.		Bering Strait transitioning from closed to open.	Open Bering Strait/closed CAA: more liquid freshwater into the Nordic Seas.			Fresher subpolar NA in SSP126 (Kwiatkowski et al., 2020), The liquid freshwater export increases in the Fram Strait in SSP245 (Zanowski et al., 2021).
Temperature over Norway ⁸	No data	Warm	Warm	Cold	Warm	Cold	
Wind	Assumed northern shift of the mid-latitude westerly jet, related to the overall warmer North Atlantic SSTs (inferred from PlioMIP (3.258 Ma time slice) findings (Li et al., 2015)).						The projection of the midlatitude atmospheric circulation is highly uncertain in SSP585 (Oudar et al., 2020).

¹ See Fig. S1. Strength refers to relative relation between Pliocene states. ² For Pliocene, the %NADW is calculated following (Bell et al., 2015). The indicated strengths are presented relative to Pliocene mean (ca 62%NADW). See Fig. S2 and Table S1 for Pliocene background information and dataset references. ³ Not from CMIP6. ⁴ Ventilation indicated relative to Pliocene mean. For further details see Fig. S2. ⁵ See Fig. S3 and S4 for Pliocene background data. ⁶ See Fig. S5 for Pliocene background data for assessment of tropical change. *Data not available from all sites. ⁷ Information about Pliocene sea ice occurrence and extent is extracted from (Clotten et al., 2018; Clotten et al., 2019; Knies et al., 2014). Relative sea ice relation between intervals is indicated by +/- . The references to more/less liquid freshwater refer to a relative relation between Pliocene states. ⁸ Based on data from Panitz et al. (2018). See Fig. S6 for further information.



455 We also note that minor geographical differences exist between the Pliocene and the present and future. The Greenland
Scotland Ridge was deeper by a few hundred meters (Poore et al., 2006), the Canadian Arctic Archipelago was closed
(Matthiessen et al., 2009) and the Barents Sea was most likely subaerial (Butt et al., 2002). These differences were,
however, constant through the investigated time interval and would therefore not impact the interpretation of our results.
In contrast, the Bering Strait opened during the investigated time interval and is suggested to have altered the Arctic
460 freshwater balance and consequently the Nordic Seas oceanography (Table 2) (De Schepper et al., 2015; Otto-Bliesner et
al., 2016). The consequences of the opening of the Bering Strait on the buoyancy forcing is therefore considered.

The in-phase situation is addressed in Section 4.1. The Iceland Sea being out of phase with the North Atlantic and
Norwegian Sea is addressed in Section 4.2, and the situation when the North Atlantic is out of phase with the Iceland and
465 Norwegian Seas is addressed in Section 4.3. The situation where the Norwegian Sea is out of phase with both the North
Atlantic and the Iceland Sea is not seen in any of the idealized experiments. This case will be discussed in Section 4.4.

4.1 All regions in-phase

An in-phase relation between SST anomalies of the North Atlantic, Norwegian and Iceland Seas is seen at multidecadal
470 time scales in the HadISST dataset (Fig. 6 and 7) and over three Pliocene time intervals covering hundreds of thousands
of years, from 5.23-5.03 Ma, 4.65-4.43 Ma and 4.33-4.03 Ma (Fig. 9). In the observation-based record the in-phase
relationship is linked to the continuous northward propagation of heat anomalies from the subpolar region and towards
the Arctic, taking about 5-10 years to propagate north with a frequency of about 14 years (Árthun et al., 2017). In-phase
is also seen for more than half of the Pliocene time interval considered in this study, and therefore we consider the in-
475 phase situation to be the norm also for Pliocene climate, reflecting the connection of the three regions by ocean circulation
(Fig. 1).

Warm SST anomalies characterized the two oldest Pliocene in-phase intervals while the youngest Pliocene in-phase
interval was a cold SST anomaly situation. During the warm in-phase intervals the overturning circulation, as derived
480 from the % North Atlantic Deep Water (%NADW) (Table 2), was somewhat stronger than the Pliocene mean. However,
the intermediate depth ventilation of the Norwegian Sea was weaker than the Pliocene mean (Table 2). During the cold
in-phase interval, neither the overturning circulation nor the intermediate depth ventilation of the Norwegian Sea deviated
from its mean Pliocene condition (Table 2). In line with a weaker overturning circulation during the cold in-phase interval
relative to the warm in-phase intervals, a stronger North Atlantic meridional SST gradient and somewhat enhanced fresh
485 water forcing, characterized the cold in-phase anomalies relative to the warm anomalies of the Pliocene (Table 2). From
the idealized experiments the in-phase relationship is seen under weak precipitation perturbations over the Nordic Seas,
under constant SSTs (Table 1; Fig. 10b). Nonsignificant responses are seen for all selected output parameters from the
idealized experiments (Table 1); which seems consistent with no change in the ocean circulation during the cold Pliocene
in-phase interval.

490

The time scale considered for the observations and the Pliocene reconstructions are very different (multidecadal versus
hundreds of thousands of years), however, we consider both to reflect equilibrium, or quasi-equilibrium, responses. The
time scales involved in either case is longer than the propagation-driven lag that sets up the anti-phase relation at
interannual time scales. Compared to the future scenarios which undergo transient changes due to strong external forcing
495 we regard the era of instrumental observations to be in quasi-equilibrium. The Pliocene reconstructions represent the



predominant situation over hundreds of thousands of years. Higher frequency variability did take place superimposed on these predominant features, e.g., exemplified by orbital-scale variability visible in the original raw datasets (Fig. 2). Multidecadal-scale variability is however not resolved for any of the relevant Pliocene sites, and the existing age constraints would not have been good enough to investigate phase relations at such time scales, or at orbital scales. While
500 not a focus for this study, we note that the amplitude of the Pliocene SST anomalies, from about 1°C to close to 3°C, is larger than the observation-based anomalies that are mostly less than 0.5°C (Fig. 6 and 9). The difference in amplitude of the observed and Pliocene anomalies may in part be influenced by the different time scales.

The main difference between the warm and cold in-phase periods in the Pliocene was a somewhat stronger fresh water influence during the cold in-phase interval, inferred from the occurrence of the sea ice marker IP₂₅ in the Iceland Sea (Clotten et al., 2019) and that the Bering Strait was fully opened (De Schepper et al., 2015) (Table 2). While there exists evidence for sea ice in the Arctic and the Iceland Sea, it is important to note that the Arctic sea ice extent was considerable smaller than today throughout the Pliocene (Clotten et al., 2019; Knies et al., 2014). Since the Canadian Arctic Archipelago (Fig. 1) was closed throughout the Pliocene (Matthiessen et al., 2009), the Fram Strait was the only Arctic
510 Ocean exit. Opening the Bering Strait allowed for inflow of Pacific water with a lower salinity to the Arctic Ocean, and consequently, enhanced transport of fresh water from the Arctic Ocean to the Nordic Seas (Hu et al., 2015). Sensitivity experiments performed with CCSM4 have shown that a closed Canadian Arctic Archipelago entails colder SSTs in the North Atlantic, Norwegian and Iceland Seas relative to the PlioMIP1 experiments where both the Bering Strait and the Canadian Arctic Archipelago were open (Otto-Bliesner et al., 2016). In the idealized experiments an (insignificant) cold
515 in-phase response is found with weak to intermediate freshwater forcing (precipitation over the Nordic Seas). We therefore suggest that the increase in freshwater reaching the Nordic Seas from the Arctic Ocean may have caused the cold in-phase case. We acknowledge that the source and distribution of freshwater is not directly comparable between the Pliocene and the idealized experiments: The precipitation change in the MITgcm experiments are distributed equally over the Nordic Seas basin, while the sea ice and liquid freshwater transported from the Arctic Ocean to the Nordic Seas at
520 any time during the Pliocene likely followed the boundary current along the east Greenland margin. Less fresh water was available in the region during the warm Pliocene in-phase intervals, also in line with the idealized experiments where an (insignificant) warm in-phase response is seen for a weak salinity increase (Table 1; Fig. 10b).

4.2 The Iceland Sea out of phase with the North Atlantic and the Norwegian Sea

525 A warm anomaly in the Iceland Sea corresponding with no change in the North Atlantic and the Norwegian Sea is documented for the Pliocene, between 3.43 and 3.23 Ma (Fig. 9). Hence, this SST field was present for hundreds of thousands of years. During this time, there are indications of a weakened overturning circulation (smaller %NADW contribution) relative to the Pliocene mean (Table 2), despite the Norwegian Sea being well ventilated down to intermediate depths (Risebrobakken et al., 2016) (Table 2). In line with a weakened overturning circulation, a strong
530 North Atlantic meridional SST gradient existed, due to the relatively cold North Atlantic and Norwegian Sea. While the Arctic Sea ice cover was still smaller than today (Knies et al., 2014), constant, rather than emerging, existence of IP₂₅ in the Iceland Sea (Clotten et al., 2018) suggests more available fresh water in the form of spring sea ice, relative to the in-phase intervals (Table 2). The idealized experiments show that weak atmospheric warming under constant precipitation (G1 to REF-1 and G1 to REF-3) are consistent with a positive Iceland Sea SST anomaly out of phase with, or strictly
535 speaking no change in, the North Atlantic and the Norwegian Sea SSTs (Table 1; Fig. 10a and c). These idealized experiments are associated with a reduction in all selected output parameters, relative to the respective reference experiment; the density gradient between the northern and southern basin, velocity of the inflow over the sill, velocity of



the Norwegian Sea boundary current, heat transport over the sill and in the maximum overturning streamfunction at the sill.

540

While not directly comparable, the overall reduction of the overturning at the sill in the idealized experiment seems consistent with a reduced %NADW for this period in the Pliocene (Table 2). A weakened ocean circulation brings less heat and salt into the Norwegian Sea and by continuation the Iceland Sea. In the Iceland Sea, the presence of seasonal sea ice may enhance the freshening caused by a weakened inflow of Atlantic water to the Nordic Seas, and thereby strengthen the stratification. How this should result in a warm Iceland Sea SST anomaly is, however, not clear. In the idealized experiments, an Iceland Sea out of phase scenario is also obtained through strongly increased freshwater forcing under constant atmospheric temperatures (P4 to REF-2). However, the resulting response is then a cold SST anomaly in the Iceland Sea and warm anomalies in the North Atlantic and the Norwegian Sea, the opposite situation of what is seen by the Pliocene reconstructions (Fig. 6, 8 and 9).

550

As mentioned above, the idealized experiment that does reproduce the documented phase relation with a warm Iceland Sea SST anomaly corresponding with a cold SST anomaly in the North Atlantic and the Norwegian Sea is associated with an equally distributed weak warming over the full Nordic Seas (Table 1 and Fig. 10a and c; G1 to REF-1 and G1 to REF-3). Pliocene air temperatures for the Nordic Seas domain are, however, largely unknown. No information exists from Iceland (Verhoeven et al., 2013). Over Norway, colder air temperature is indicated between 3.43 and 3.23 Ma, mirroring the colder Norwegian Sea SSTs (Table 2) (Panitz et al., 2018), but contrasting the weak warming that from the idealized experiments explains the reconstructed SST phase relation.

555

Hence, from the idealized experiments we manage to set up the warm Iceland Sea cold North Atlantic and Norwegian Sea anomaly scenario. However, the link between the reconstructed background climate and oceanography and the comparable output parameters from the idealized experiments are not straight forward, emphasizing the need for further studies.

560

4.3 The North Atlantic out of phase with the Norwegian and Iceland Seas

At multidecadal time scales a positive SST change (warming) in the Norwegian and Iceland Seas corresponding with a small (close to zero) negative SST change (cooling) in the North Atlantic is seen in CMIP6 future projections, depending on the scenario used (Fig. 8). While global SSTs are overall higher for the SSP126 scenario, and the tropical SSTs are up to 2°C warmer (Table 2), the subpolar North Atlantic cools, and freshens (Kwiatkowski et al., 2020). For SSP245 increased export of liquid freshwater is seen in the Fram Strait (Zanowski et al., 2021). The AMOC is weak compared to the historical level for all CMIP6 scenarios (Weijer et al., 2020) (Table 2). A similar phase relation emerges in the idealized experiments for an intermediate to strong atmospheric warming over the Nordic Seas, under constant precipitation (Table 1 and Fig. 10; G2-G4 to REF-1 and G2 to REF-3). All these increasing temperature experiments are associated with a reduction in the heat transport over the sill, the maximum overturning streamfunction at the sill, the velocity of the Norwegian Sea boundary current and the density gradient between the northern and southern basin, relative to respective reference experiments.

570

575

The time scales involved when looking at the future is comparable to the observational record, both addressing SST variability at multidecadal time scales. The discussed phase relation with the Iceland Sea and Norwegian Sea being out of phase with the North Atlantic is, however, part of a transient response to an imposed CO₂ forcing. Strictly speaking



580 this case is therefore not representative for an equilibrium or quasi-equilibrium situation, as discussed for all the other
phase relations.

The same phase relation as found in the CMIP6 future scenario runs are previously identified for CMIP5 future projections
(Alexander et al., 2018; Nummelin et al., 2017) and in the Grand Ensemble of the MPI-ESM1.1 climate model (Keil et
585 al., 2020). Keil et al. (2020) shows that the heat import to the North Atlantic, associated with a weakening of the low
latitude AMOC, decreases consistently, in parallel to an increased heat transport over the sill set up by a corresponding
change in the high latitude overturning and the subpolar gyre circulation, in line with Alexander et al. (2018) and
Nummelin et al. (2017). However, after 80 years of simulation time, they see a stall, followed by a small gradual decrease,
in the ocean heat transport over the sill. As described above, our idealized experiments show that the phase relation, with
590 the North Atlantic out of phase with the other two regions, is associated with a reduced heat transport over the sill, which
appears to be opposite to the results from simulated future projections. We stress again that the result from the idealized
experiments refers to equilibrium conditions whereas the CMIP5/6 future projections show transient changes to external
forcing, and thus, have not reach an equilibrium. This is exemplified by the results from Keil et al. (2020), where the
ocean heat transport over the sill is first increasing and then slightly decreasing. Therefore, we find it hard to conclude on
595 what is causing this phase relation.

Independent of the exact cause, the indirect effects of both a strong increase in atmospheric CO₂ concentrations (CMIP5/6
future projections) and increased atmospheric temperatures over the Nordic Seas (idealized experiments) may break the
in-phase expectation and set up an out of phase SST relation between the SST anomalies in the North Atlantic (cold) and
600 the Norwegian and Iceland Seas (warm).

A similar phase relation did not take place during the investigated Pliocene time interval. However, we find it interesting
that despite the large differences in time scales involved, multidecadal versus hundreds of thousands of years, the strongest
SST anomaly seen in the future (up to 2°C between 2068 and 2098 for the Norwegian and Iceland Seas in CNRM-ESM2-
605 1; Fig. 8) are comparable to the amplitude of the Pliocene SST anomalies (Fig. 9), both larger than the amplitude of the
anomalies seen in the instrumental observations (less than 0.8°C; Fig. 6). The amplitude of the future changes depends
both on the chosen model and scenario; these large anomalies are seen for SSP126 in CNRM-ESM2-1 and for SSP585 in
NorESM. The CO₂ forcing of SSP126 is comparable to the high end of the Pliocene CO₂ range (Meinshausen et al., 2020;
De La Vega et al., 2020), proposing an indirect link between radiative forcing and strength of the SST anomalies of the
610 North Atlantic and the Nordic Seas.

4.4 The Norwegian Sea out of phase with the North Atlantic and the Iceland Sea

At two times during the Pliocene, 3.63-3.93 Ma and 4.73-4.93 Ma, the Norwegian Sea SSTs was out of phase with both
the Iceland Sea and the North Atlantic (Fig. 9). Between 4.73 and 4.93 Ma a cold SST anomaly was seen in the Norwegian
615 Sea, contemporary with a warm anomaly in the Iceland Sea and the North Atlantic. The younger period, 3.63 to 3.93 Ma,
represents the opposite situation, with a warm Norwegian Sea anomaly corresponding to a cold SST anomaly in the
Iceland Sea and the North Atlantic (Fig. 9). During both periods, the %NADW was close to the Pliocene mean strength
(Table 2; Fig. S2). For both cases the intermediate depth Norwegian Sea ventilation was stronger than in the in-phase
periods, and even stronger when the Norwegian Sea was warm, relative to the Pliocene mean (Table 2). The main
620 difference between the cold (4.73 to 4.93 Ma) and warm (3.63 to 3.93 Ma) Norwegian Sea anomaly situations was that
more freshwater entered the Nordic Seas from the Arctic Ocean in the warm scenario, following the opening of the Bering



Strait, and that traces of sea ice was present in the Iceland Sea (Table 2). In addition, the Norwegian Sea intermediate and upper water column ventilation was stronger during the warm anomaly situation. None of our idealized experiments resulted in a phase relation where the Norwegian Sea is out of phase with the other two regions.

625

Hence, we look further into this case from a conceptual point of view. Two main oceanographic features hold the potential to change the expected in-phase equilibrium behaviour between the three locations; a change in ocean circulation and advective pathways that weaken the advective interlinkage, or a change in water column stratification at a site, e.g., related to an anomalous influx of surface freshwater. A change in the advective pathway could for example be the case if the Iceland Sea could remain downstream of Atlantic Water, but more under the influence of the Irminger Current entering directly through the Denmark Strait rather than the water eventually reaching the Iceland Sea via the Norwegian Atlantic Current. Or if the surface water in the Iceland Sea is more under influence of the East Greenland Current and thus the Polar domain, a situation that also could relate to a stratification change in the Iceland Sea.

630

635 Following this conceptual framework, a cold SST anomaly in the Norwegian Sea corresponding with a warm North Atlantic and Iceland Sea SST anomaly may result from a weakened Norwegian Atlantic Current compensated by a strong Irminger Current. More of the North Atlantic warm water will then enter the Iceland Sea from southwest rather than into the Norwegian Sea in the east. Based on existing information we cannot verify if this was the case, or not, between 4.73 and 4.93 Ma.

640

In contrast, the existence of a warm anomaly in the Norwegian Sea corresponding with cold anomalies in the North Atlantic and in the Iceland Sea could in theory result from a strengthened or expanded East Greenland Current, increasing the fraction of cold polar water reaching the Iceland Sea and the North Atlantic. The existence of sea ice in the Iceland Sea (Clotten et al., 2019), combined with the effect of enhanced fresh water supply from the Arctic as a response to the fully opened Bering Strait (De Schepper et al., 2015) (Table 2), may support such a scenario. This interval was quite similar to the cold in-phase situation (Section 4.1), except that the cold in-phase case was associated with a higher %NADW and weaker ventilation of the upper Norwegian Sea water column. We suggest that changes in the Arctic freshwater balance, and consequently a strengthened East Greenland Current and/or stratification of the Iceland Sea, may be a likely scenario for the cold Iceland Sea and North Atlantic and warm Norwegian Sea anomaly case. In the MITgcm setup used, freshwater forcing is induced by precipitation change evenly spread over the Nordic Seas and the ocean currents in the interior basin are not very well represented (e.g., the Irminger Current). Combined, this may explain why we do not detect this phase relation through the idealized experiments. Alternatively, even stronger forcing might be needed to set up a similar response for the idealized experiments.

645

650

655 **5 Summary and future avenues**

Through our analysis of observation-based data (from year 1870 AD), CMIP6 projections of the next century and Pliocene SST reconstructions covering the time interval between 5.23 and 3.13 Ma, we have identified four occurring phase relations between the North Atlantic, Norwegian and Iceland Seas SSTs (Fig. 11): 1) All regions in-phase (observations and Pliocene; warm and cold in-phase anomalies). 2) The Iceland Sea being out of phase with the North Atlantic and the Norwegian Sea (Pliocene; warm Iceland Sea and cold North Atlantic and Norwegian Sea). 3) The North Atlantic being out of phase with the Norwegian and Iceland Seas (future scenarios; cold North Atlantic and warm Norwegian and Iceland Seas). 4) The Norwegian Sea being out of phase with the North Atlantic and the Iceland Sea (warm and cold Norwegian Sea corresponding with a cold and warm North Atlantic and Iceland Sea, respectively).

660



665 We show that an out of phase relation emerges in the low (ssp126) (and intermediate (ssp585)) future emission scenarios and are not limited to the high emission scenarios. Whether the out of phase relation is seen in the low emission scenario or not is, however, dependent on the model's equilibrium climate sensitivity. It is most pronounced in the most sensitive model (CNRM-ESM2-1).

670 Furthermore, we show that occurrence of out of phase relation is independent of the transient nature of the future scenario runs. Different out of phase relations occurred during the Pliocene, when the background climate is considered to have been in equilibrium with a CO₂ forcing comparable to the present atmospheric concentrations and the SSP126 scenario. While the documented phase relations take place over a range of different time scales, the phase relations based on observation and reconstruction, as well as the idealized experiments, represent equilibrium, or quasi-equilibrium, situations. The future change is in that sense the odd case, reflecting a transient response to a given CO₂ forcing.

The idealized MITgcm experiments, set up to investigate the impact of buoyancy forcing, reproduce three out of four of the documented phase relations (Table 1, Fig. 10 and 11). An in-phase relationship is seen as a response to a weak to intermediate freshwater forcing, under constant atmospheric temperatures. As the SAT or precipitation forcing increases, 680 the Iceland Sea gets out of phase with the North Atlantic and the Norwegian Sea. Under even stronger forcing, both the Norwegian and Iceland Seas get out of phase with the North Atlantic. The situation with a warm SST anomaly in the Iceland Sea and cold anomalies in the North Atlantic and Norwegian Sea is the result of a weak atmospheric warming over the Nordic Seas. A stronger atmospheric warming over the Nordic Seas sets up the cold North Atlantic warm Norwegian and Iceland Seas scenario.

685 Based on the idealized experiments and reviewed information about global SSTs, overturning circulation and ventilation of the Nordic Seas, the Atlantic Ocean equator-pole SST gradient and freshwater forcing, we find that: The in-phase situation is the norm relative to the mean background climate state under weak forcing. The situation when the Iceland Sea is out of phase with the Norwegian Sea and the North Atlantic likely reflect a response to a weakened ocean 690 circulation. The situation where the North Atlantic is out of phase with the Norwegian and Iceland Sea occur in association with warmer air temperatures caused by increased atmospheric CO₂ concentrations.

The case when the Norwegian Sea is out of phase with the North Atlantic and the Iceland Sea, observed for two Pliocene intervals, cannot be explained by the idealized experiments. Here we suggest that a weakened NwAC compensated by a strong Irminger Current in theory could set up a cold Norwegian Sea anomaly at the same time as the North Atlantic and 695 Iceland Sea experienced a warm SST anomaly. The opposite situation, with a warm Norwegian Sea and cold North Atlantic and Iceland Sea SST anomalies, may be linked to an expanded East Greenland Current, increasing the fraction of cold polar water reaching the Iceland Sea. Both more data and further sensitivity studies are needed to settle the discussion on this specific phase relation.

700 The amplitude of the SST variability is overall larger during the Pliocene than in the observational record. The largest amplitude seen for future multidecadal SST changes in the Norwegian and Iceland Seas is more comparable to the amplitude of the Pliocene SST variability. Why this is the case is out of the scope of this paper and will need to be explored further in future studies. However, since both the Pliocene reconstructions and the future change occur under atmospheric



705 CO₂ concentrations around 400 ppm or higher, these results indicates that the amplitudes of SST anomalies in the Nordic
Seas depends on the radiative forcing.

Acknowledgement

We acknowledge support from the Centre for Climate Dynamics at the Bjerknes Centre for Climate Research and RCN
710 projects No 221712 and 229819. The model simulations were performed on resources provided by UNINETT Sigma2 -
the National Infrastructure for High Performance Computing and Data Storage in Norway, project NN9709K. The CMIP6
analysis is part of the IS-ENES3 project that has received funding from the European Union's Horizon 2020 research and
innovation program under grant agreement No 824084.

References

- 715 Alexander, M. A., Scott, J. D., Friedland, K. D., Mills, K. E., Nye, J. A., Pershing, A. J., and Thomas, A. C.: Projected sea surface
temperatures over the 21st century: Changes in the mean, variability and extremes for large marine ecosystem regions of Northern
Oceans, *Elem. Sci. Anth.*, 6, 9. DOI:<https://doi.org/10.1525/elementa.1191>, 2018.
- Bachem, P., Risebrobakken, B., and McClymont, E. L.: Sea surface temperature variability in the Norwegian Sea during the late
720 Pliocene linked to subpolar gyre and radiative forcing, *Earth and Planetary Science Letters*, 446, 113-122, 2016.
- Bachem, P. E., Risebrobakken, B., De Schepper, S., and McClymont, E. L.: Highly variable Pliocene sea surface conditions in the
Norwegian Sea, *Clim. Past.*, 13, 1153-1168, <https://doi.org/1110.5194/ep-1113-1153-2017>, 2017.
- Bartoli, G., Hönisch, B., and Zeebe, R. E.: Atmospheric CO₂ decline during the Pliocene intensification of Northern Hemisphere
glaciations, *Paleoceanography*, 26, PA4213, doi:4210.1029/2010PA002055, 2011.
- 725 Bell, D. B., Jung, S. J. A., Kroon, D., Hodell, D. A., Lourens, L. J., and Raymo, M. E.: Atlantic Deep-water Response to the Early
Pliocene Shoaling of the Central American Seaway, *Scientific Reports*, 5, 12252, doi:12210.11038/srep12252, 2015.
- Blindheim, J. and Østerhus, S.: The Nordic Seas, Main Oceanographic Features, in: *The Nordic Seas: An integrated Perspective*,
edited by: Drange, H., Dokken, T., Furevik, T., Gerdes, R., and Berger, W., Geophysical Monograph Series, American Geophysical
Union, Washington DC, 11-38, 2005.
- 730 Bourke, R. H., Weigel, A. M., and Paquette, R. G.: The Westward Turning Branch of the West Spitsbergen Current, *Journal of
Geophysical Research*, 93, 14065-14077, 1988.
- Bringedal, C., Eldevik, T., Skagseth, Ø., Spall, M., and Østerhus, S.: Structure and forcing of observed exchanges across the
Greenland-Scotland Ridge, *Journal of Climate*, 31, 9881-9901, doi.org/9810.1175/JCLI-D-9817-0889, 2018.
- Butt, F. A., Drange, H., Elverhøi, A., Otterå, O. H., and Solheim, A.: Modelling Late Cenozoic isostatic elevation changes in the
735 Barents Sea and their implications for oceanic and climatic regimes: preliminary results, *Quaternary Science Reviews*, 21, 1643-
1660, 2002.
- Cheng, W., Chiang, J. C. H., and Zhang, D.: Atlantic Meridional Overturning Circulation (AMOC) in CMIP5 models: RCP and
Historical Simulations, *Journal of Climate*, 24, 7187-7197, 2013.
- Clotten, C., Stein, R., Fahl, K., and De Schepper, S.: Seasonal sea ice cover during the warm Pliocene: Evidence from the Iceland
740 Srea (ODP Site 907), *Earth and Planetary Science Letters*, 481, 61-72, <https://doi.org/10.1016/j.epsl.2017.1010.1011>, 2018.
- Clotten, C., Stein, R., Fahl, K., Schreck, M., Risebrobakken, B., and De Schepper, S.: On the causes of Sea Ice in the warm Early
Pliocene, *Scientific Reports*, 9:989, <https://doi.org/910.1038/s1598-1018-37047-y>, 2019.
- de la Vega, E., Chalk, T. B., Wilson, P. A., Bysani, R. P., and Foster, G. L.: Atmospheric CO₂ during the Mid-Piacenzian Warm
Period and the M2 glaciation, *Scientific Reports*, 10, 11002, <https://doi.org/11010.11038/s41598-11020-67154-11008>, 2020.
- 745 De Schepper, S., Schreck, M., Beck, K. M., Matthiessen, J., Fahl, K., and Mangerud, G.: Early Pliocene onset of modern Nordic Seas
circulation related to ocean gateway changes, *Nature Communication*, 6:8659 doi:8610.1038/ncomms9659, 2015.
- DeRepentigny, P., Jahn, A., Holland, M. M., and Smith, A.: Arctic sea ice in two configurations of the CESM2 during the 20th and
21st centuries, *Journal of Geophysical Research: Ocean*, 125, e2020JC016133, <https://doi.org/016110.011029/012020JC016133>,
2020.



- 750 Dowsett, H., Dolan, A., Rowley, D., Muoucha, R., Forte, A. M., Mitrovica, J. X., Pound, M. J., Salzmann, U., Robinson, M.,
Chandler, M., Foley, K., and Haywood, A.: The PRISM4 (mid-Piacenzian) paleoenvironmental reconstruction, *Clim. Past.*, 12, 1519-
1538, 15.5194/cp-12-1519/2016, 2016.
- Drijfhout, S., van Olderborg, G. T., and Cimatoribus, A.: Is a decline of AMOC causing the warming hole above the North Atlantic
in observed and modeled warming patterns?, *Journal of Climate*, 25, 8373-8379, doi:<https://doi.org/8310.1029/2012GL052459>.
- 755 2012.
- Furevik, T., Drange, H., and Sorteberg, A.: Anticipated changes in the Nordic Seas marine climate: Scenarios for 2020, 2050, and
2080, *Fisken og Havet*, 4, <http://hdl.handle.net/11250/113241>, 2002.
- Furevik, T., Mauritzen, C., and Ingvaldsen, R.: The flow of Atlantic Water to the Nordic Seas and Arctic Ocean, in: *Arctic-Alpine
Ecosystems and People in a Changing Environment*, edited by: Ørbæk, J. B., Kallenborn, R., Tombre, I., Nøst Hegseth, E., Falk-
760 Petersen, S., and Hoel, A. H., Springer, 123-146, 2007.
- Herbert, T. D., Lawrence, K. T., Tzanova, A., Peterson, L. C., Caballero-Gill, R., and Kelly, C. S.: Late Miocene global cooling and
the rise of modern ecosystems, *Nature Geoscience*, 9, 843-849, 2016.
- Holliday, N. P., Hughes, S. L., Bacon, S., Beszczynska-Möller, A., Hansen, A. W., Lavin, H., Loeng, H., Mork, K. A., Østerhus, S.,
Sherwin, T., and Walczowski, W.: Reversal of the 1960s to 1990s freshening trend in the northeast North Atlantic and Nordic Seas,
765 *Geophysical Research Letters*, 35, L03614, 2008.
- Hu, A., Meehl, G. A., Han, W., Otto-Bliesner, B., Abe-Ouchi, A., and Rosenbloom, N.: Effects of the Bering Strait closure on
AMOC and global climate under different background climates, *Progress in Oceanography*, 132, 174-196,
<http://dx.doi.org/110.1016/j.pocean.2014.1002.1004>, 2015.
- IPCC (Ed.) *Climate Change 2021: The Physical Science Basis. Contribution of Working Group I to the Sixth Assessment Report of
770 the Intergovernmental Panel on Climate Change*, Cambridge University Press, 2021.
- Jackett, D. R. and McDougall, T. J.: Minimal adjustment of hydrographic profiles to achieve static stability., *J. Atmos. Oceanic
Technol.*, 12, 381–389, 1995.
- Jansen, E., Fronval, T., Rack, F., and Channell, J. E. T.: Pliocene-Pleistocene ice rafting history and cyclicity in the Nordic Seas
during the last 3.5 Myr, *Paleoceanography*, 15, 709-721, 2000.
- 775 Keil, P., Mauritsen, T., Jungclaus, J., Hedemann, C., Olonschenck, D., and Ghosh, R.: Multiple drivers of the North Atlantic
warming hole, *Nature Climate Change*, 10, 667-671, 2020.
- Knies, J., Cabedo-Sanz, P., Belt, S. T., Baranwal, S., Fietz, S., and Rosell-Melé, A.: The emergence of modern sea ice cover in the
Arctic Ocean, *Nature Communication*, 5, doi:10.1038/ncomms6608, 2014.
- Knight, J. R., Allan, R. J., Folland, C. K., BVellinga, M., and Mann, M. E.: A signature of persistent natural thermohaline circulation
780 cycles in observed climate, *Geophysical Research Letters*, 32, L20708, doi:20710.21029/22005GL024233, 2005.
- Kwiatkowski, L., Torres, O., Bopp, L., Aumont, O., Chamberlain, M., Christian, J. R., Dunne, J. P., Gehlen, M., Ilyina, T., John, J.
G., Lenton, A., Li, H., Lovenduski, N. S., Orr, J. C., Palmieri, J., Santana-Falcón, Y., Schwinger, J., Séférian, R., Stock, C. A.,
Tagliabue, A., Takano, Y., Tjiputra, J., Toyama, K., Tsujino, H., Watanabe, M., Yamamoto, A., Yool, A., and Ziehn, T.: Twenty-first
century ocean warming, acidification, deoxygenation, and upper-ocean nutrient and primary production decline from CMIP6 model
785 projections, *Biogeosciences*, 17, 3439–3470, <https://doi.org/3410.5194/bg-3417-3439-2020>, 2020.
- Lawrence, K. T., Herbert, T. D., Brown, C. W., Raymo, M., and Haywood, A. M.: High-amplitude variations in North Atlantic sea
surface temperature during the early Pliocene warm period, *Paleoceanography*, 24, PA2218, doi:2210.1029/2008PA001669, 2009.
- Li, X., Jiang, D., Zhang, Z., Zhang, R., Tian, Z., and Yan, Q.: Mid-Pliocene Westerlies from PlioMIP Simulations, *Advances in
Atmospheric Sciences*, 32, 909-923, 2015.
- 790 Locarini, R. A., Mishonov, A. V., Baranova, O. K., Boyer, T. P., Zweng, M. M., Garcia, H. E., Reagan, J. R., Seidov, D., Weathers,
K., Paver, C. R., and Smolyar, I.: *World Ocean Atlas 2018, Volume 1: Temperature*, 52, 2018.
- Macrander, A., Valdimarsson, H., and Jónsson, S.: Improved transport estimate of the East Icelandic Current 2002-2012, *Journal of
Geophysical Research: Oceans*, 119, 3407-3424, doi:3410.1002/2013JC009517, 2014.
- Marshall, J., Hill, C., Perelman, L., and Adcroft, A.: Hydro-static, quasi-hydrostatic, and non-hydrostatic ocean modeling, *Journal of
795 Geophysical Research*, 102, 5733–5752, 1997.



- Matthiessen, J., Knies, J., Vogt, C., and Stein, R.: Pliocene paleoceanography of the Arctic Ocean and subarctic seas, *Phil. Trans. R. Soc. Lond. A*, 367, 21-48, 2009.
- Mauritzen, C.: Production of dense overflow waters feeding the North Atlantic across the Greenland-Scotland Ridge. Part 1: Evidence for a revised circulation scheme., *Deep Sea Research I*, 43, 769-837, 1996.
- 800 Meehl, G. A., Senior, C. A., Eyring, V., Flato, G., Lamarque, J.-F., Stouffer, R. J., Taylor, K. E., and Schlund, M.: Context for interpreting equilibrium climate sensitivity and transient climate response from the CMIP6 Earth system models, *Science Advances*, 6, eaba1981, <https://doi.org/10.1126/sciadv.aba1981>, 2020.
- Meinshausen, M., Nicholls, Z. R. J., Lewis, J., Gidden, M. J., Vogel, E., Freund, M., Beyerle, U., Gessner, C., Nauels, A., Bauer, N., Canadell, J. G., Daniel, J. S., John, A., Krummel, P. B., Luderer, G., Meinshausen, N., Montzka, S. A., Rayner, P. J., Reimann, S., 805 Smith, S. J., van den Berg, M., Velders, G. J. M., Vollmer, M. K., and Wang, R. H. J.: The shared socio-economic pathway (SSP) greenhouse gas concentrations and their extensions to 2500, *Geosci. Model Dev.*, 13, 3571–3605, <https://doi.org/3510.5194/gmd-3513-3571-2020>, 2020.
- Müller, P. J., Kirst, G., Ruhland, G., Vvon Storch, I., and Rosell-Melé, A.: Calibration of the alkenone paleotemperature index UK'37 based on core tops from the eastern South Atlantic and the global ocean (60°N-60°S), *Geochemica et Cosmochemica Acta*, 810 62, 1757-1772, 1998.
- Nummelin, A., Li, C., and Hezel, P. J.: Connecting ocean heat transport changes from the midlatitudes to the Arctic Ocean, *Geophysical Research Letters*, 44, doi:10.1002/2016GL071333, 2017.
- Otto-Bliesner, B., Jahn, A., Feng, R., Brady, E. C., Hu, A., and Löffverström, M.: Amplified North Atlantic warming in the late Pliocene by changes in Arctic gateways, *Geophysical Research Letters*, 44, doi:10.1002/2016GL071805, 2016.
- 815 Oudar, T., Cattiaux, J., and Douville, H.: Drivers of the Northern Extratropical Eddy-Driven Jet Change in CMIP5 and CMIP6 Models, *Geophysical Research Letters*, 47, e2019GL2086 2695, <https://doi.org/2010.1029/2019GL086695>, 2020.
- Paillard, D., Labeyrie, L., and Yiou, P.: Macintosh program performs time-series analysis, *EOS, Trans. AGU, TI*, 379, 1996.
- Panitz, S., Salzmann, U., Risebrobakken, B., De Schepper, S., Pound, J. M., Haywood, A., Dolan, A. M., and Lunt, D.: Orbital, tectonic and oceanographic control of Pliocene climate and atmospheric circulation in Arctic Norway, *Global Planetary Change*, 161, 820 183-193, 2018.
- Poore, H. R., Samworth, R., White, N. J., Jones, S. M., and McCave, I. N.: Neogene overflow of Northern Component Water at the Greenland-Scotland Ridge, *Geochem Geophys Geosy*, 7, Artn Q06010, Doi 06010.01029/02005gc001085, 2006.
- Rayner, N. A., Parker, D. E., Horton, E. B., Folland, C. K., Alexander, L. V., Rowell, D. P., Kent, E. C., and Kaplan, A.: Global analyses of sea surface temperature, sea ice, and night marine air temperature since the late nineteenth century, *Journal of* 825 *Geophysical Research Atmosphere*, doi:10.1029/2002JD002670, 2003.
- Risebrobakken, B., Andersson, C., De Schepper, S., and McClymont, E. L.: Low-frequency Pliocene climate variability in the eastern Nordic Seas, *Paleoceanography*, 31, doi:10.1002/2015PA002918, 2016.
- Ryan, W. B. F., Carbotte, S. M., Coplan, J., O'Hara, S., Melkonian, A., Arko, R., Weissel, R. A., Ferrini, V., Goodwillie, A., Nitsche, F., Bonczkowski, J., and Zemsky, R.: Global Multi-Resolution Topography (GMRT) synthesis data set, *Geochem. Geophys. Geosyst.*, 10, Q03014, doi:03010.01029/02008GC002332, 2009.
- 830 Seland, Ø., Bentsen, M., Graff, L. S., Olivié, D., Toniazzo, T., Gjermundsen, A., Debernard, J. B., Gupta, A. K., He, Y., Kirkevåg, A., Schwinger, J., Tjiputra, J., Aas, K. S., Bethke, I., GFan, Y., Griesfeller, J., Grini, A., Guo, C., Ilicak, M., Karseth, I. H. H., Landgren, O., Liakka, J., Moseid, K. O., Nummelin, A., Spensberger, C., Tang, H., Zhang, Z., Heinze, C., Iversen, T., and Schulz, M.: Overview of the Norwegian Earth System Model (NorESM2) and key climate response of CMIP6 DECK, historical, and 835 scenario simulations, *Geosci. Model Dev.*, 13, 6165-6200, <https://doi.org/6110.5194/gmd-6113-6165-2020>, 2020.
- Smagorinsky, J.: General circulation experiments with the primitive equations: I. The basic experiment, *Mon. Wea. Rev.*, 91, 99-164, 1963.
- Smetsrud, L. H., Muilwijk, M., Brakstad, A., Madonna, E., Lauvset, S. K., Spensberger, C., Born, A., Eldevik, T., Drange, H., Jeansson, E., Li, C., Olsen, A., Skagseth, O., Slater, D. A., Straneo, F., Våge, K., and Árrthun, M.: Nordic Seas Heat Loss, Atlantic 840 Inflow, and Arctic Sea Ice Cover Over the Last Century, *Review of Geophysics*, 60, e2020RG000725, doi.org/10.1029/2020RG000725, 2022.



- Spall, M. A.: On the role of eddies and surface forcing in the heat transport and overturning circulation in marginal seas, *J. Climate*, 24, 4844–4858, <https://doi.org/4810.1175/2011JCLI4130.4841>, 2011.
- Spall, M. A.: Influences of precipitation on water mass transformation and deep convection, *Journal of Physical Oceanography*, 42, 1684–1700, <https://doi.org/1610.1175/JPO-D-1611-0230.1681>, 2012.
- 845 Talley, L. D., Pickard, G. L., Emery, W. J., and Swift, J. H.: Chapter 5 - Mass, Salt, and Heat Budgets and Wind Forcing, in: *Descriptive Physical Oceanography (Sixth Edition)*, edited by: Talley, L. D., Pickard, G. L., Emery, W. J., and Swift, J. H., Academic Press, 111-145, doi.org/110.1016/C2009-1010-24322-24324, 2011.
- Verhoeven, K., Louwye, S., and Eiriksson, J.: Plio-Pleistocene landscape and vegetation reconstruction of the coastal area of the 850 Tjörnes Peninsula, Northern Iceland, *Boreas*, 42, 108-122, 2013.
- Wei, T., Yan, Q., Qi, W., Ding, M., and Wang, C.: Projections of Arctic sea ice conditions and shipping routes in the twenty-first century using CMIP6 forcing scenarios, *Environ. Res. Lett.*, 15, 104079, <https://doi.org/104010.101088/101748-109326/abb104072c104078> 2020.
- Weijer, W., Cheng, W., Garuba, O. A., Hu, A., and Nadiga, B. T.: CMIP6 models predict significant 21st century decline of the 855 Atlantic meridional overturning circulation, *Geophysical Research Letters*, 47, <https://doi.org/10.1029/2019GL086075> 2020.
- Zanowski, H., Jahn, A., and Holand, M. M.: Arctic Ocean Freshwater in CMIP6 Ensembles: Declining Sea ice, Increasing Ocean Storage and Export, *Journal of Geophysical Research: Ocean*, 126, e2020JC016930, <https://doi.org/016910.011029/012020JC016930>, 2021.
- Årthun, M. and Eldevik, T.: On Anomalous Ocean Heat Transport toward the Arctic and Associated Climate Predictability, *Journal of Climate*, 29, 689-704, 2016.
- 860 Årthun, M., Eldevik, T., Viste, E., Drange, H., Furevik, T., Johnson, H. L., and Keenlyside, N.: Skillful prediction of northern climate provided by the ocean, 8, 15875, doi:15810.11038/ncomms15875, 2017.